NPR

Cite this: *Nat. Prod. Rep.*, 2012, **29**, 87

www.rsc.org/npr

REVIEW

The diazofluorene antitumor antibiotics: Structural elucidation, biosynthetic, synthetic, and chemical biological studies

Seth B. Herzon* and Christina M. Woo

Received 24th June 2011
DOI: 10.1039/c1np00052g

Covering: up to 2011

This review presents a comprehensive survey of all aspects of the kinamycins and lomaiviticins, potent antiproliferative antimicrobial metabolites isolated from various strains of *Streptomyces* and *Salinispora*. The kinamycins and lomaiviticins contain a diazotetrahydrobenzo[*b*]fluorene (diazofluorene) functional group, which is unique among known natural products. This review begins with an account of the studies leading to the final (correct) structure determination of the kinamycins, which were originally proposed to contain an *N*-cyano carbazole function. This is followed by a discussion of biosynthetic studies, which established the polyketide nature of the kinamycins. Descriptions of four completed syntheses of various kinamycins, synthetic studies toward the lomaiviticins, syntheses of the carbohydrates of the lomaiviticins, and syntheses of structurally-related metabolites, are then presented. A survey of chemical biological investigations, including *in vitro* reactivity studies, which indicate that the kinamycins and lomaiviticins may form reactive *ortho*-quinone methide or free radical intermediates *in vivo*, is presented. Finally, a selection of structurally-related metabolites are described.

1 Introduction and isolation
2 Structure elucidation
2.1 The kinamycins
2.2 The lomaiviticins
3 Biosyntheses of the kinamycins
4 Syntheses of the kinamycins
4.1 Enantioselective synthesis of (−)-kinamycin C (Porco and Lei)
4.2 Synthesis of (±)-*O*-methyl-kinamycin C (Ishikawa and co-workers)
4.3 Enantioselective syntheses of kinamycins C, F, and J (Nicolaou and co-workers)
4.4 Enantioselective synthesis of (−)-kinamycin F (Herzon and co-workers)
5 Synthetic studies toward the lomaiviticins
5.1 Introduction
5.2 Syntheses of dimeric core structures (Nicolaou and co-workers)
5.3 Synthesis of the C-3/C-3′-dideoxy lomaiviticin core (Sulikowski and co-workers)
5.4 Synthesis of the complete lomaiviticin carbon skeleton (Shair and co-workers)
5.5 Synthesis of the monomeric unit of the lomaiviticin aglycon (Nicolaou and co-workers)
5.6 Synthesis of the lomaiviticin aglycon (Herzon and co-workers)
6 Syntheses of the lomaiviticin carbohydrates and glycosylation studies
6.1 Introduction
6.2 Synthesis of the pyrrolosamine residue and the direct formation of β-2-deoxyglycosides by *O*-alkylation (Shair and co-workers)
6.3 Synthesis of *N*,*N*-dimethyl-pyrrolosamine and oleandrose. Incorporation into a lomaiviticin model system (Herzon and co-workers)
7 Syntheses of metabolites related to the kinamycins and lomaiviticins
7.1 Introduction
7.2 Prekinamycin (original and revised structures; Hauser, Echavarren, Birman, and Ishikawa groups)
7.3 Isoprekinamycin (Dmitrienko and co-workers)
7.4 Kinobscurinone (Snieckus and co-workers)
7.5 Stealthins (Gould and Kamikawa groups)
8 Chemical biological studies
8.1 Introduction
8.2 Chemical biological studies of the kinamycins and lomaiviticins (Melander, Hasinoff, and Dimitrienko groups)

Yale University – Chemistry, 225 Prospect Street, P.O. Box 208107, New Haven, Connecticut, 06520-8107, United States

8.3 *In vitro* reactivity studies (Jebaratnam, Dmitrienko, Feldman, Skibo, and Moore groups)
9 Related metabolites
9.1 Introduction
9.2 Momofulvenones
9.3 Seongomycin
10 Conclusion and outlook
11 References and notes

1 Introduction and isolation

The kinamycins and lomaiviticins are complex bacterial metabolites that were isolated from various strains of *Streptomyces* and *Salinispora*.[1] Owing to the presence of a common diazotetrahydrobenzo[*b*]fluorene substructure, these metabolites are often referred to as "diazofluorenes" (*vide infra*). Kinamycins A–D (**1–4**, Table 1) are the earliest known members of this family. They were isolated by Ōmura and co-workers as yellow or orange needles from a strain of *Streptomyces murayamaensis*, itself obtained from a soil sample in Murayama, Saitama-ken, Japan.[2–5] Subsequently, many different kinamycins have been isolated, and these are differentiated primarily by the acylation pattern about the D-ring (Table 1).[6–11] All of the metabolites in Table 1 are levorotatory, with the exception of kinamycins E (**5**) and I (**9**), whose optical rotation does not appear to have been determined.

Table 1 Structures of kinamycins A–J (**1–10**)

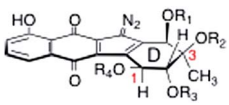

kinamycin	R_1	R_2	R_3	R_4	Ref.
(−)-A (**1**)	H	Ac	Ac	Ac	2–5
(−)-B (**2**)	H	Ac	H	H	2–5
(−)-C (**3**)	Ac	H	Ac	Ac	2–5
(−)-D (**4**)	Ac	H	Ac	H	2–5
E (**5**)	Ac	H	H	H	6,8
(−)-F (**6**)	H	H	H	H	6,8
(−)-G (**7**)	Ac	C(O)*i*-Pr	Ac	Ac	7
(−)-H (**8**)	C(O)*i*-Pr	H	Ac	Ac	7
I (**9**)	C(O)*i*-Pr	H	C(O)*i*-Pr	Ac	9
(−)-J (**10**)	Ac	Ac	Ac	Ac	2–5

The related dimeric metabolites lomaiviticins A and B (**11** and **12**) were isolated by He and co-workers in 2001 (Fig. 1).[12] The lomaiviticins bear some structural homology to the kinamycins, but important differences exist between the two classes of natural products. Most notably, the lomaiviticins possess two monomeric diazofluorenes united by a carbon–carbon bond [and in the case of lomaiviticin B (**12**), two carbon–oxygen bonds], to form a C_2-symmetric structure. The naphthoquinone substructure of the lomaiviticins incorporates two hydroxyl groups (rather than a single hydroxyl group, as in the kinamycins), the tertiary alcohol functions (C-3) of the lomaiviticins possess an ethyl substituent (rather than methyl, as in the kinamycins), the C-1 position of the lomaiviticins are at the carbonyl oxidation state (rather than the alcohol oxidation state, as in the kinamycins), and the periphery of the lomaiviticins are functionalized with 2–4 2,6-dideoxyglycoside residues, oleandrose and *N*,*N*-dimethylpyrrolosamine (rather than acyl substituents, as in the kinamycins).

The relationship between lomaiviticins A (**11**) and B (**12**) is, at present, not known. Given the hydrolytic instability of 2-deoxyglycosides,[13] it is conceivable that lomaiviticin B (**12**) may arise from lomaiviticin A (**11**) by hydrolysis of the oleandrose residues (see structure **14**) followed by cyclization (Scheme 1). Alternatively, lomaiviticin B (**12**) may be a biosynthetic precursor to lomaiviticin A (**11**) by direct glycosylation, or the two may diverge from a common intermediate earlier in the biosynthetic pathway.

Structurally, the kinamycins and lomaiviticins contain a diazocyclopentadiene fused to an oxygenated naphthoquinone and a partially unsaturated six-membered ring. This substructure constitutes a diazotetrahydrobenzo[*b*]fluorene (see structure **13**, Fig. 1), and these metabolites are often referred to as diazofluorenes. Because the diazofluorene macrofunctional group was

Seth B. Herzon

Seth B. Herzon was born in Philadelphia, Pennsylvania in 1979. He received his BS in Chemistry from Temple University (2002) and his PhD from Harvard University (2006), under the guidance of Professor Andrew G. Myers. From 2006–2008 he was a postdoctoral fellow in the laboratory of Professor John F. Hartwig at the University of Illinois, Urbana–Champaign. In 2008, he began his independent career at Yale University. His research focuses on natural products synthesis.

Christina M. Woo

Christina Woo was born in Syracuse, New York in 1986. She received her BA in Chemistry from Wellesley College (2008). In 2008, she began graduate studies at Yale University in the laboratory of Professor Seth Herzon. Her research focuses on synthetic and chemical biological studies of the kinamycins, lomaiviticins, and unnatural diazofluorene-based anticancer agents.

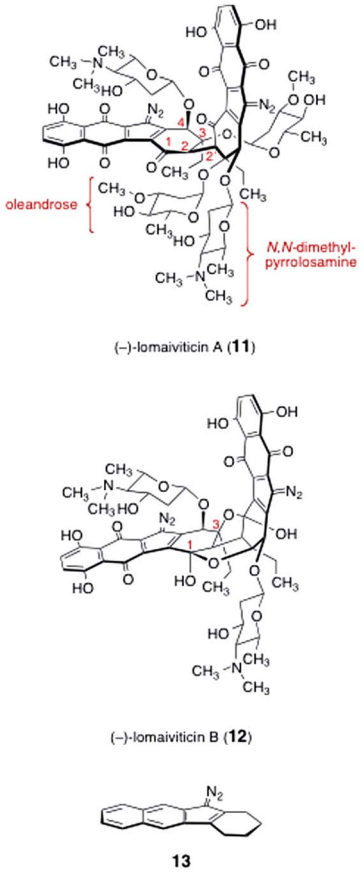

Fig. 1 Structures of lomaiviticin A (**11**), lomaiviticin B (**12**), and diazotetrahydrobenzo[*b*]fluorene (**13**).

unprecedented in natural products, the structural elucidation of the kinamycins was not straightforward (*vide infra*). The extended π-conjugation of the diazofluorene, coupled with the peripheral oxygen substituents, makes it difficult to predict the reactivity of the constituent functionality. From a synthetic standpoint, this generates many exciting questions relating to stability, reagent compatibility, and strategy.

The kinamycins and lomaiviticins are potent anticancer agents, with 50 percent inhibitory potencies at nanomolar–picomolar concentrations. The activity profiles of kinamycin C (**3**)[14] and lomaiviticin A (**11**)[12] are unique, suggesting a novel mechanism of action is operative. Both the kinamycins and lomaviticins have shown activity against Gram-positive and Gram-negative bacteria.[12]

Reviews of the kinamycins,[15,16] diazo-containing natural products,[17] and diazo-based anticancer agents[18] have been previously published. This review seeks to cover all aspects of the chemistry and biology of the diazofluorene antitumor antibiotics, including the lomaiviticins, with an emphasis on synthetic and chemical biological research conducted since 2000.

2 Structure elucidation

2.1 The kinamycins

The structure elucidation of the kinamycins was a formidable challenge, and the pathway from isolation to structure

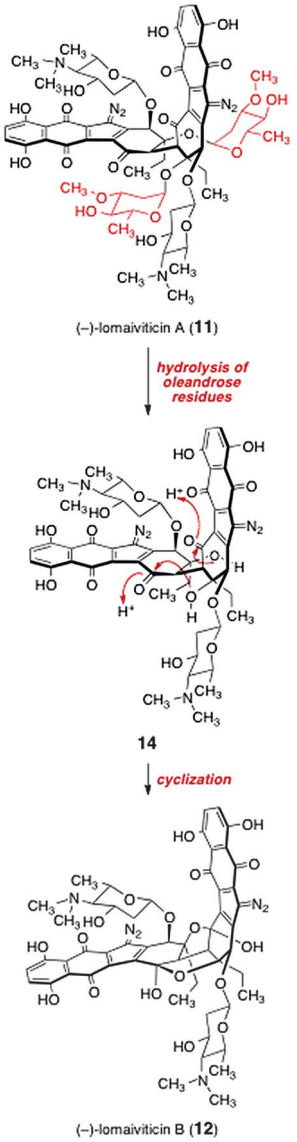

Scheme 1 Potential mechanism for the conversion of lomaiviticin A (**11**) to lomaiviticin B (**12**).

determination involved the work of several research groups over a period of more than twenty years. The structural elucidation was challenging, in part, because at the time the kinamycins were isolated, high field NMR instruments and proton-detected multidimensional pulse sequences were not widely available. Moreover, the D-ring and juglone fragments of the kinamycins are separated by a large number of quaternary carbon atoms, preventing correlation of these spin systems by $^{3}J_{H}$ couplings. Perhaps most significantly, closely related compounds, which would be useful as benchmarks for spectroscopic comparison, were not well-known. As will be shown, the originally proposed structure for the kinamycins contained a cyanamide rather than a diazo function. Subsequent investigations led to permutation of the cyanamide atoms to a diazo function. This pathway from isolation to determination of the correct structure is described below.

Initial spectroscopic and degradation studies of the kinamycins were conducted by Ōmura and co-workers in the early

1970s.[2–5] These investigations established the constitution and relative stereochemistry of the D-ring and the juglone fragments of the kinamycins. Based on MS and IR analysis (strong absorption at ~2150 cm^{-1}), and the results of alkaline degradation (liberation of ammonia), a cyanamide function was suggested to bridge the juglone and D-ring substructures, leading to a unique *N*-cyanocarbazole function (**15**, Fig. 2). Shortly thereafter, an X-ray analysis of a *para*-bromobenzoate derivative of kinamycin C (**3**) was obtained, which established the absolute stereochemistry.[19] However, the quality of the X-ray data did not permit rigorous assignment of the putative cyanamide function. Instead, the presence of this function was inferred based on Ōmura's earlier studies. It was noted[20] that the carbon-13 resonance of the putative cyanamide carbon of kinamycin D (**4**) was not observed. This was attributed to an unusually long relaxation time or obfuscation by other signals.

In the late 1980s and early 1990s, the results of several studies began to generate uncertainty surrounding the *N*-cyanocarbazole. In 1988, Gould demonstrated that fermentation of *Streptomyces murayamaensis* in the presence of $(^{15}NH_4)_2SO_4$ produced [$^{15}N_2$]-kinamycin D.[21] The putative cyanamide carbon was unequivocally identified by distinct C, N couplings in the proton-decoupled carbon-13 NMR spectrum. This carbon resonated at δ 78.5 (dd, $J_{C,N}$ = 21.2, 5.4 Hz). Careful re-inspection of ^{13}C NMR data of natural kinamycin D (**4**) revealed a small singlet at the same resonance, nearly obscured by the chloroform-d signal. Gould noted that this chemical shift was *ca.* 30 ppm upfield of typical cyanamide resonances.

In 1990, Dmitrienko and co-workers reported the synthesis and characterization of a series of *N*-cyanoindoloquinones, as exemplified by structure **16** (Fig. 2).[22] These workers observed that the resonance of the cyanamide carbon was in the $\delta \sim 105$ range, as expected based on literature precedent. Additionally, the cyanamide infrared stretch of **16** was in the 2237–2259 cm^{-1} range, *vs.* 2119–2170 cm^{-1} for the kinamycins.

In 1993, Echavarren and co-workers reported the preparation of structure **17**,[23] which was referred to as prekinamycin (itself isolated[6,8] from the producing strain of the kinamycins). The cyanamide carbon of Echavarren's synthetic material (**17**) was observed at $\delta \sim 112$, clearly distinct from the shift reported for natural prekinamycin (δ 83.7).[8] ^1H spectroscopic data of synthetic and natural prekinamycin were also incongruent. Collectively, these studies called into question the original structural assignment of prekinamycin and the kinamycins.

The matter was finally settled in 1994 in back-to-back communications by Gould[24] and Dmitrienko.[25] Gould presented two critical data points. First, he showed that treatment of natural prekinamycin with dirhodium tetracetate in methanol yielded the fluorene **19** (Scheme 2). The location of the newly formed vinyl proton (H-1, δ 7.25) was established by observation of an NOE to H-2 and a $^3J_{C,H}$ coupling to the semiquinone phenolic carbon. In parallel, his research group obtained a high-quality crystal structure of the (+)-α-methylbutyrate of kinamycin D. The refined data set was shown to best accommodate a diazo group, rather than a cyanamide or isonitrile function. Contemporaneously, Dmitrienko prepared a wholly synthetic derivative of prekinamycin and showed that spectroscopic data of the synthetic material were significantly different than that of natural prekinamycin. It was shown that ^{13}C NMR and IR spectroscopic data for the kinamycins agree best with those of known diazofluorenes, such as 9-diazofluorene. The Dmitrienko group also noted that the nitrogen coupling constants of [$^{15}N_2$]-kinamycin D[21] ($J_{N,N}$ = 3.4 Hz, $^1J_{C,N}$ = 21.2 Hz, $^2J_{C,N}$ = 5.4 Hz) were similar to those of [$^{15}N_2$]-ethyldiazoacetate ($J_{N,N}$ = 5.7 Hz, $^1J_{C,N}$ = 20.4 Hz, $^2J_{C,N}$ = 5.4 Hz) and that the nitrogen chemical shifts of [$^{15}N_2$]-kinamycin D[21] (δ 241.6, 344.6) were similar to known diazo compounds (δ 227–287, δ 332–441).

As a result of these careful investigations the structure of the kinamycins and prekinamycin were reassigned as diazotetrahydrobenzo[*b*]fluorenes[24,25] (diazofluorenes; correct structures shown in Table 1 and Scheme 2), a substructure that, like the *N*-cyanoindole originally proposed, was without close analogy in natural products chemistry.

2.2 The lomaiviticins

The lomaiviticins were isolated as amorphous red powders from the fermentation broth of a bacteria originally classified as *Micromonospora lomaivitiensis*[12] (subsequently reclassified as *Salinispora*).[1] Analysis of the mass spectrometry data, as well as proton and carbon-13 NMR spectra, led He and co-workers to

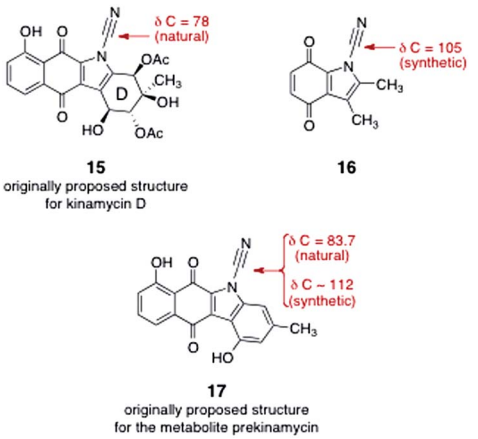

Fig. 2 Kinamycin D [**15**, original (incorrect) structure], *N*-cyanoindoloquinone **16**, and prekinamycin [**17**, original (incorrect) structure].

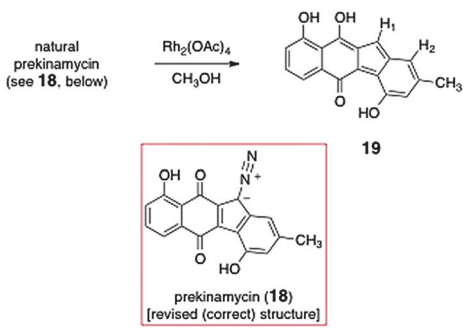

Scheme 2 Rhodium-catalyzed cleavage of the diazo function of prekinamycin (**18**).

propose a C_2-symmetric dimeric structure with the molecular formula of $C_{68}H_{80}N_6O_{24}$ for lomaiviticin A (**11**). Extensive multidimensional NMR analyses were used to establish connectivity and relative stereochemistry. The connectivity of the bis(cyclohexenone) core of lomaiviticin A (**11**) was determined by HMBC and HMQC analysis. A w-coupling between H-2 and H-4 in the COSY spectrum necessitated that these protons be *syn*-disposed (Fig. 1). The location of the bridging carbon–carbon bond was determined by HMBC and HMQC analysis: a cross-peak from H-2 to C-2/C-2′ was observed in both the HMBC and HMQC spectra, establishing the location of this key bond. The presence of carbohydrate residues – *N*,*N*-dimethylpyrrolosamine[26] and oleandrose – was revealed, and the relative (but not absolute) stereochemistry of these carbohydrates, including the stereochemistry of the glycoside linkages, was elucidated by analysis of $^3J_{H,H}$ coupling constants. The location of the aminosugar was established by observation of an HMBC correlation from H-4 to the anomeric carbon of the aminosugar. The remaining carbohydrate was assigned to the C-3 oxygen atom, and this was supported by observation of an ROE enhancement between the C-3 ethyl substituent and the anomeric proton of the oleandrose residue. The NMR resonances of the 5,8-dihydroxy-1,4-naphthoquinone substructure were typical. On the basis of a broadened ^{13}C NMR signal at δ 78.8, and an IR band at 2148 cm^{-1}, a diazofluorene function was assigned. These latter data agree well with those of the kinamycins (*vide supra*).

Analyses of HRMS, ^1H, and ^{13}C data for lomaiviticin B (**12**) supported the existence of a C_2-symmetric structure with a molecular formula of $C_{54}H_{56}N_6O_{18}$. In this case, the ketone resonance of lomaiviticin A (**11**, δ 198.4) was replaced by a quaternary carbon at δ 96.5. Additionally, the oleandrose residues of lomaiviticin A (**11**) were absent in the spectra of lomaiviticin B (**12**), lending support to the cyclic furanol structure of **12**. To the extent that the lomaiviticins may share similar biosynthetic pathways, the cyclic structure of lomaiviticin B (**12**) lends support to the relative stereochemical assignments of the bis(cyclohexenone) core of lomaiviticin A (**11**). The remaining diazofluorene resonances were consonant with lomaiviticin A (**11**) and the kinamycins. The absolute stereochemistry of the lomaiviticins was not established, but was assigned by analogy to that of the kinamycins. Both lomaiviticins are levorotatory.

3 Biosyntheses of the kinamycins

The biosyntheses of the kinamycins was studied extensively by Gould and co-workers. A comprehensive accounting of this work can be found in a recent review,[15] and a brief synopsis is presented here. The pathway begins with elaboration of 10 equivalents of *S*-acetylcoenzyme A to the natural product dehydrorabelomycin (**20**, Scheme 3). A novel ring contraction then occurs to form kinobscurinone (**21**).[27] As discussed above, labeling studies established that the diazo functional group is derived from ammonia. It was shown that this proceeds by a two-step process, *via* the intermediacy of the metabolite stealthin C (**22**).[28] The mechanism of the oxidation of **22** to **18** is not known. Interestingly, owing to the presence of paramagnetic valence tautomers, both kinobscurinone (**21**)[27] and stealthin C (**22**)[28] are

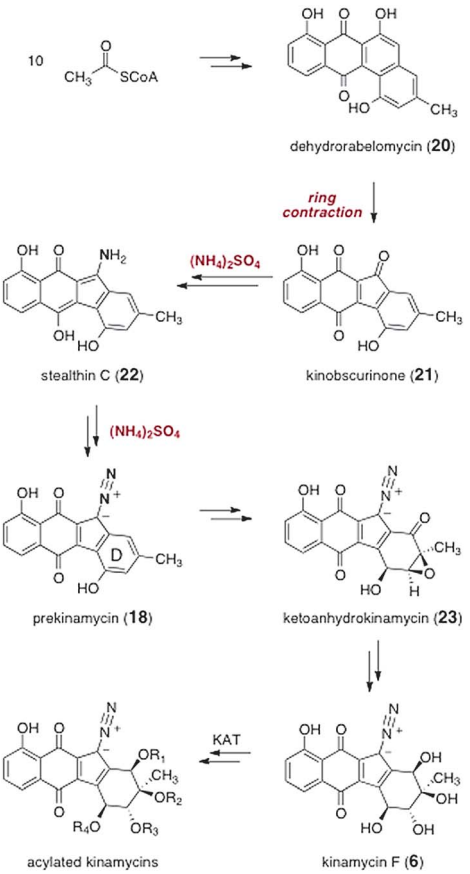

Scheme 3 Biosyntheses of the kinamycins.

NMR silent. The intermediacy of **21** and **22** in kinamycin biosyntheses have been unequivocally established by isotope-enrichment studies.[27,28]

Oxidative dearomatization of the D-ring then generates ketoanhydrokinamycin (**23**), itself a metabolite identified in fermentation broths containing the kinamycins.[8] Although the intermediacy of ketoanhydrokinamycin (**23**) in kinamycin biosynthesis has not been rigorously established, its structural homology to, and co-production with, the kinamycins makes it a likely intermediate. Finally, a sequence of oxidation state changes and rearrangements is proposed to generate kinamycin F (**6**). A biomimetic approach to the kinamycins, which hinges on the transformation of synthetic constructs resembling ketoanhydrokinamycin (**23**), has been described by Dmitrienko and co-workers.[29]

A 669 kDa multifunctional enzyme (or enzyme complex), termed kinamycin acetyltransferase 1 (KAT 1), has been identified in the final steps of kinamycin biosynthesis.[30] In cell-free experiments, KAT 1 exhibited dual acetyltransferase activity. It was shown to catalyze the acetyl coenzyme A-dependent conversion of the tetraol kinamycin F (**6**) to the monoacetate kinamycin E (**5**). KAT 1 also converted the latter to the diacetate kinamcyin D (**4**). Thus, kinamycin F (**6**) is a precursor to kinamycins D (**4**) and E (**5**), and potentially many other kinamycins, although the remaining KATs have yet to be identified.

4 Syntheses of the kinamycins

4.1 Enantioselective synthesis of (−)-kinamycin C (Porco and Lei)

In 2006, Porco and Lei reported a synthesis of (−)-kinamycin C (**3**), which constitutes the first completed route to any of the kinamycins.[31] Retrosynthetically, (−)-kinamycin C (**3**) was deconstructed to the tetracyclic ketone **24** by manipulation of the oxidation state of the naphthoquinone and cleavage of the diazo function (Scheme 4). The tetracyclic skeleton of the ketone **24** was deconstructed by Friedel–Crafts acylation and Stille coupling reactions to form the aryl stannane **25** and the vinyl bromide **26** as synthetic precursors. The aryl stannane **25** was envisioned to arise from 2-bromojuglone (**27**). The vinyl bromide was derived from the acetal **28**, itself ultimately prepared from an aromatic precursor.[32]

Porco's route to (−)-kinamycin C (**3**) began with 2,5-dihydroxybenzaldehyde (**29**), which was elaborated to the enone **26** by the sequence shown in Scheme 5. Bromination,[33] methylation, and reduction afforded the diol **30** (79% overall). Oxidation with bis(acetoxy)iodobenzene formed the quinone monoketal **32**. Protecting group manipulations then provided the acetal **33** (72%, three steps).

The authors then sought to introduce a hydroxymethylene substituent at the unsubstituted α-position of the enone **33**. This was accomplished by implementation of a modified Baylis–Hillman reaction[34] using formaldehyde as the electrophile, which formed the desired product **34** in 70% yield. Asymmetric nucleophilic epoxidation[35–37] then generated the epoxy alcohol **35** in 94% yield and 90% ee. In this reaction, it has been proposed that the sodium salt of tritylperoxide forms a 2 : 1 complex with D-di-*iso*-propyl tartrate (see structure **37**). It is believed that this complex is the active nucleophilic epoxidation reagent. Hydroxyl-directed reduction of the ketone function of **35** then afforded the alcohol **36** as a single diastereomer (90%). Finally, an efficient three-step sequence comprising mesylation of the primary alcohol function, reduction using lithium triethylborohydride (Super-Hydride®), and cleavage of the acetal afforded the enone **26** in 73% overall yield.

The synthesis of the arylstannane coupling partner **25** was accomplished by an efficient three-step sequence (Scheme 6). First, 2-bromojuglone (**27**)[38] was protected as its methoxymethyl ether derivative **38** (85%). The quinone was reduced using sodium thiosulfate, and the resulting hydroquinone was protected *in situ* with methoxymethyl chloride, to afford the arene **39** (70%). Finally, stannylation using tetrakis(triphenylphosphine)palladium and hexabutylditin[39] afforded the arylstannane coupling partner **25** in 70% yield.

Porco's pathway to complete the synthesis of (−)-kinamycin C (**3**) is shown in Scheme 7. The arylstannane **25** and the α-bromoenone **26** were efficiently coupled by a Stille reaction using tris(dibenzylideneacetone) dipalladium and triphenylarsine (70%). The coupling product (**40**) was reduced with high diastereoselectivity using Super-Hydride®, to afford the diol intermediate **41** (80%). To establish the tertiary alcohol function of the kinamycin D-ring, the epoxide of **41** was opened regioselectively using tetramethylammonium acetate and titanium tetraisopropoxide as mediator, to afford the acetate **43** in good yield and high diastereoselectivity. These epoxide-opening conditions were originally developed by Sharpless and co-workers for the regiocontrolled opening of 2,3-epoxy alcohols.[40] It was proposed that ligand exchange of the substrate with isopropoxide forms a covalently-bound substrate–titanium complex (**42**). Nucleophilic attack on this complex at the 3-position is favored over attack at the 2-position. In the case of **41**, this model would suggest binding of the C-1 hydroxyl group to the titanium center, followed by attack at the 3-position. Under these conditions, where the weak nucleophile acetate is present, steric considerations may also favor attack at the 3-position of the epoxy alcohol functionality of **41**. An added virtue of this approach is that it delivers the oxygenation with the acetate functionality required for synthesis of (−)-kinamycin C (**3**) in place.

With the D-ring of the target established, Porco and Lei focused on completion of the tetracyclic framework and installation of the diazo function. Following protection of the secondary alcohols as their corresponding acetates, the silyl ether was cleaved and the resulting primary alcohol was oxidized to the carboxylic acid **44** by a two-step sequence (59%, four steps). To close the fourth and final ring, the acid **44** was treated with trifluoroacetic anhydride in dichloroethane. Under these conditions, the acid may be activated to form a mixed anhydride, which undergoes ionization to form an acylium ion that is trapped by the electron-rich aromatic ring. Rearomatization then forms the tetracyclic ketone **24** in high yield (90%).

The methoxymethyl ether protecting groups of **24** were then cleaved using carbon tetrabromide in *iso*-propanol. The resulting hydroquinone function was oxidized by palladium on carbon

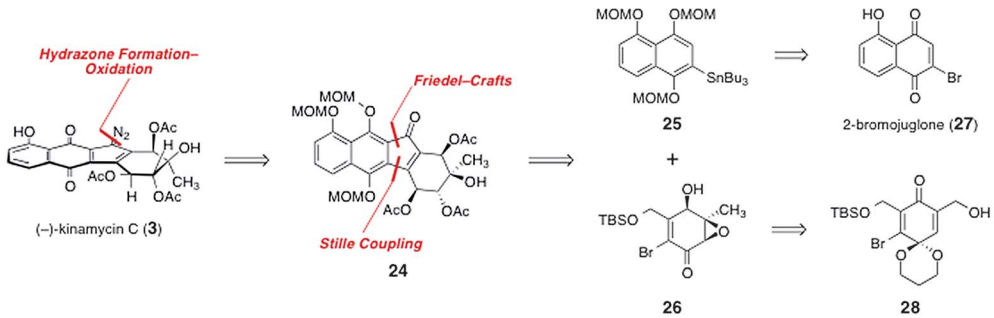

Scheme 4 Porco's retrosynthetic analysis of (−)-kinamycin C (**3**).

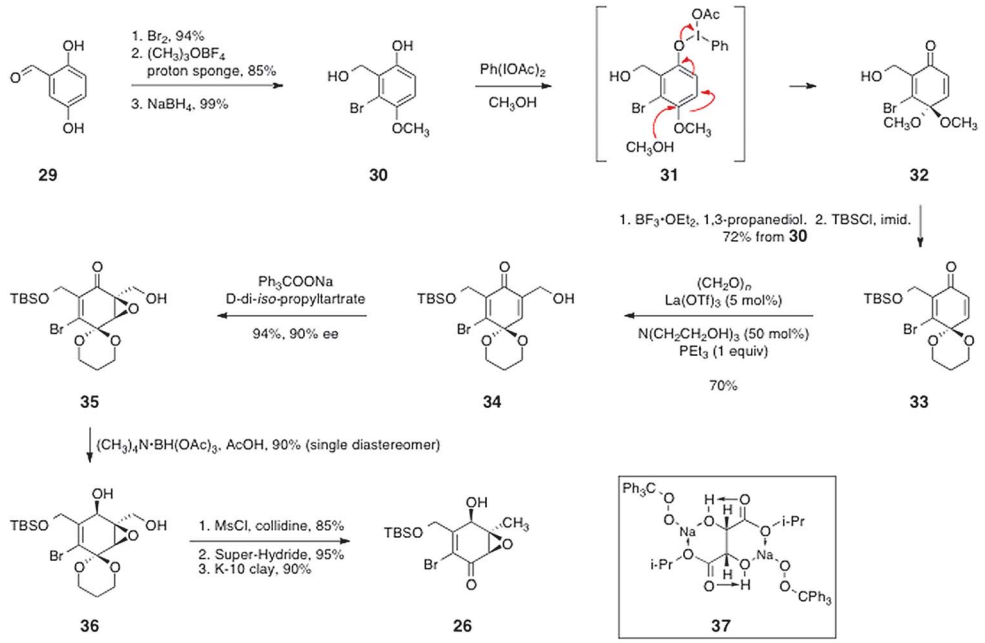

Scheme 5 Porco's synthesis of the enone **26**.

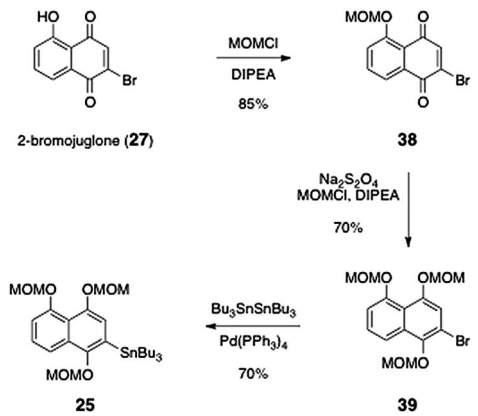

Scheme 6 Porco's synthesis of the stannane **25**.

under an atmosphere of air to afford the quinone **45** (70%, two steps). Installation of the diazo function was completed by a two-step procedure. First, the ketone function of **45** was condensed with *N*,*N*′-bis(*tert*-butyldimethylsilyl)hydrazine in the presence of scandium triflate,[41] which formed the *N*-*tert*-butyldimethylsilyl hydrazone **46**. The hydrazone **46** was then oxidized using difluoroiodobenzene[42] to afford (−)-kinamycin C (**3**) in 35% yield from **45**.

4.2 Synthesis of (±)-*O*-methyl-kinamycin C (Ishikawa and co-workers)

In 2007, Ishikawa and co-workers reported a synthesis of (±)-*O*-methylkinamycin C (**47**).[43,44] As shown in Scheme 8, the authors envisioned that **47** could be derived from the α-hydroxyindanone **48** by installation of the diazo substituent and oxidation state manipulations. The α-hydroxyindanone **48** was anticipated to arise from the enoxysilane **49**. The latter could be formed by an *endo*-selective Diels–Alder reaction between the indenone **51** and the diene **52** (see transition state **50**).

The synthesis of the indenone **51** is shown in Scheme 9.[43] Beginning with 1,5-dihydroxynapthalene (**53**), acylation with acetic anhydride formed 1,5-diacetoxynapthalene (**54**, 89%). Oxidation using *N*-bromosuccinimide in a mixture of acetic acid and water[38,45] formed *O*-acetyl-2-bromojuglone (**55**, 84%). The methyl ether **56** was then obtained by a two-step sequence comprising hydrolysis of the acetate ester and methylation of the resulting phenol with iodomethane in the presence of silver oxide (65%, two steps). The quinone function of **56** was reduced with stannous chloride and the resulting hydroquinone was methylated to form the aryl bromide **57** (77%, two steps). Lithium–halogen exchange followed by trapping with *N*,*N*-dimethylformamide formed the aldehyde **58** (84%). The aldehyde product **58** was then condensed with malonic acid to afford, after decarboxylation, the α,β-unsaturated carboxylic acid **59** (93%). Finally, the olefin of **59** was reduced (H_2, Pd/C, 93%) and the resulting product **60** was cyclized using phosphorous pentoxide in the presence of methanesulfonic acid. The dihydroindenone so formed (not shown) was oxidized by heating with IBX in DMSO to give **51** (61%, two steps).[46]

The key Diels–Alder cycloaddition was effected by treating a mixture of the indenone **51** and the diene **52** (see Scheme 8) with zinc chloride in dichloromethane at −15 °C. Under these conditions, the expected *endo*-adduct **49** was formed. Treatment of the adduct **49** with camphorsulfonic acid in methanol afforded the unsaturated ketone **61**. Finally, the unsaturated ketone **61** was regioselectively oxygenated by treatment with potassium fluoride (0.1 equiv.) in methylsulfoxide under an atmosphere of

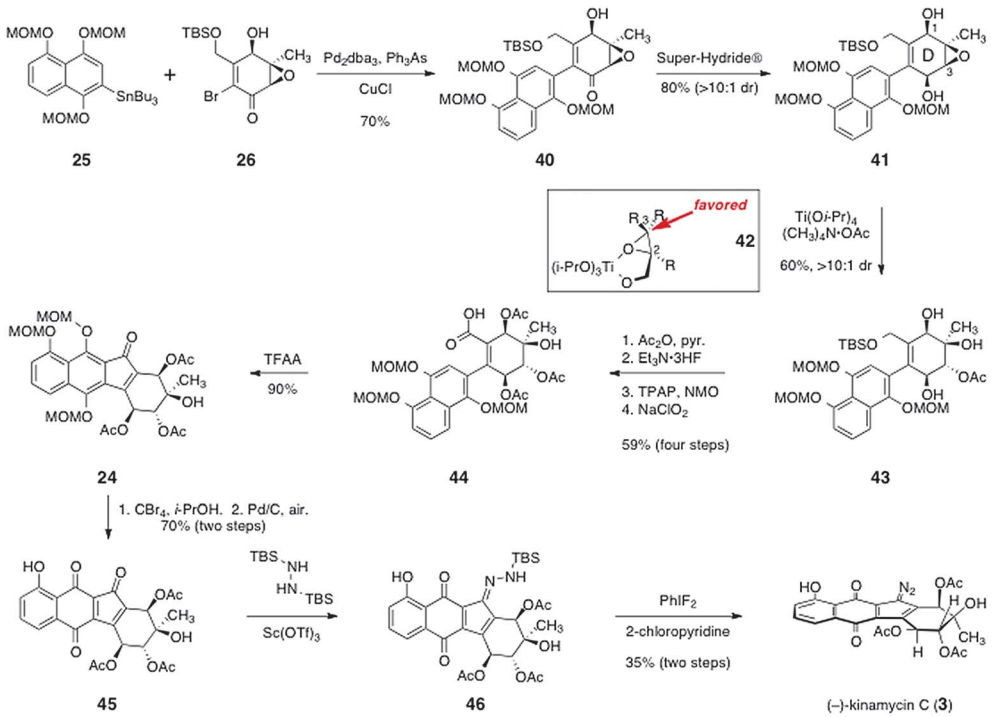

Scheme 7 Completion of the synthesis of (−)-kinamycin C (**3**) by Porco and Lei.

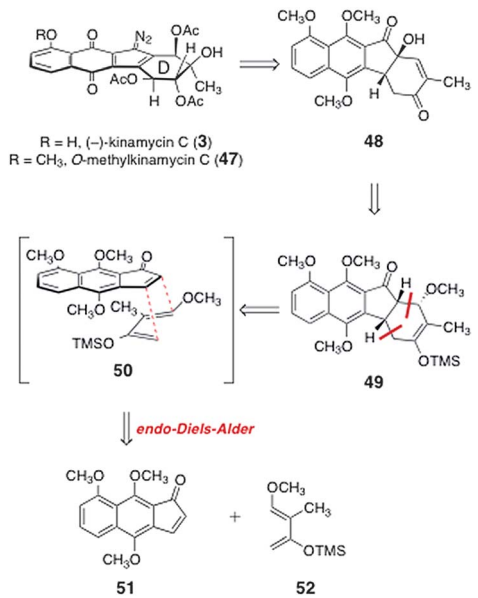

Scheme 8 Ishikawa's retrosynthesis of (±)-*O*-methyl-kinamycin C (**47**).

air. This sequence generated the tertiary alcohol **48** in 48% yield over three steps.

The final steps of Ishikawa's pathway to **47** are shown in Scheme 10. First, the allylic alcohol function of **48** was oxidized by a substrate-directed dihydroxylation reaction, as described by Donohoue and co-workers,[47] to afford the dihydroxylation product **62** (66%). The dihydroxylation product **62** was then persilylated to form the enoxysilane **63** (78%). Rubottom oxidation of **63** then generated the α-hydroxyketone **64**. The oxidation was found to occur with selectivity for the undesired α-oxidation product. Fortunately, however, this product epimerized to the desired β-epimer **65** on standing (67–71% from **63**). The silyl ether functions of **65** were then cleaved by treatment with aqueous methanol to form the tetraol **66** (91%). The secondary hydroxyl groups of **66** were selectively acylated to form the diacetate **67** (70%). The cyclohexanone function of **67** was then reduced by a diastereoselective reduction using tetramethylammonium triacetoxyborohydride.[48] Under these conditions, competitive reduction of the cyclopentanone carbonyl was also observed. Fortunately, this carbonyl could be restored by treatment with manganese dioxide, affording the desired reduction product **69** in 69% yield as a 5 : 1 mixture of diastereomers. The major diastereomer **69** likely arises from intramolecular hydride delivery of an *in situ* generated borate (see structure **68**).

The synthesis of **47** was completed by the following sequence. First, the vicinal diol function of **69** was protected as the corresponding acetonide derivative (67%, not shown). This protection step allowed for the separation of the minor diastereomer formed in the preceding reduction. Following separation, the tertiary hydroxyl group was dehydrated to form an unsaturated ketone (52%, not shown). The acetonide was then cleaved and the secondary hydroxyl groups were acylated to generate the triacetate **70** (85%). Finally, the tosylhydrazone **71** was formed by treatment of **70** with *para*-toluenesulfonylhydrazine and boron trifluoride etherate (59%). The hydrazone **71** was then oxidized using ceric ammonium nitrate. Under these conditions, the methyl ethers of the hydroquinone function were also cleaved[49] to afford **47** directly (55%).

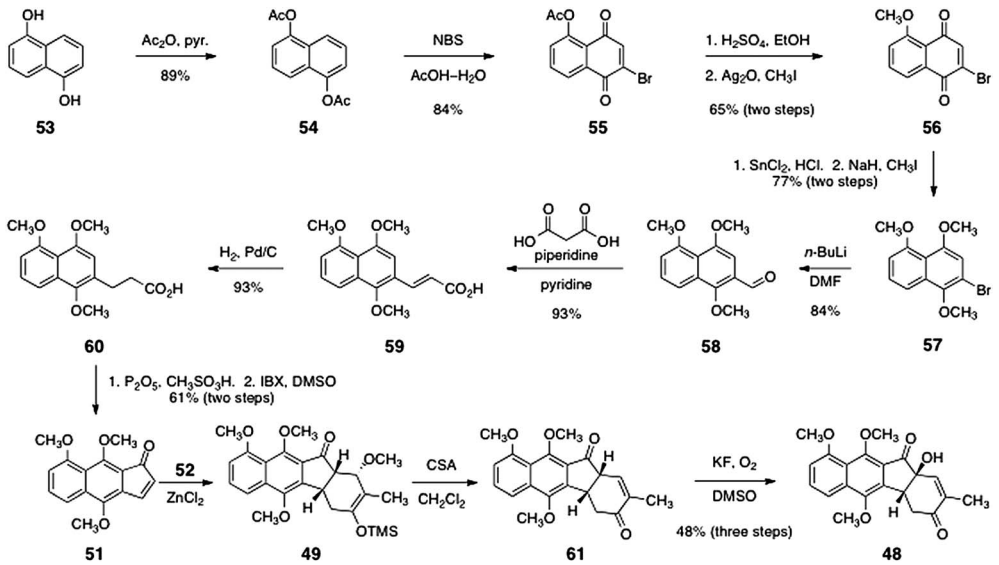

Scheme 9 Ishikawa's synthesis of the unsaturated ketone **48**.

4.3 Enantioselective syntheses of kinamycins C, F, and J (Nicolaou and co-workers)

In 2007, Nicolaou and co-workers reported efficient enantioselective syntheses of (−)-kinamycin C (**3**), (−)-kinamycin F (**6**), and (−)-kinamycin J (**10**).[50] The authors envisioned that the α-hydroxyketone **72** could serve as a precursor to the targets (Scheme 11). The α-hydroxyketone function of **72** was envisioned to arise from an Ullmann coupling–benzoin condensation sequence between the *ortho*-bromoaryl aldehyde **73** and the α-iodoenone **74**. These were derived from the bromojuglone derivative **75** and the enantiomerically enriched enone **76**, respectively.

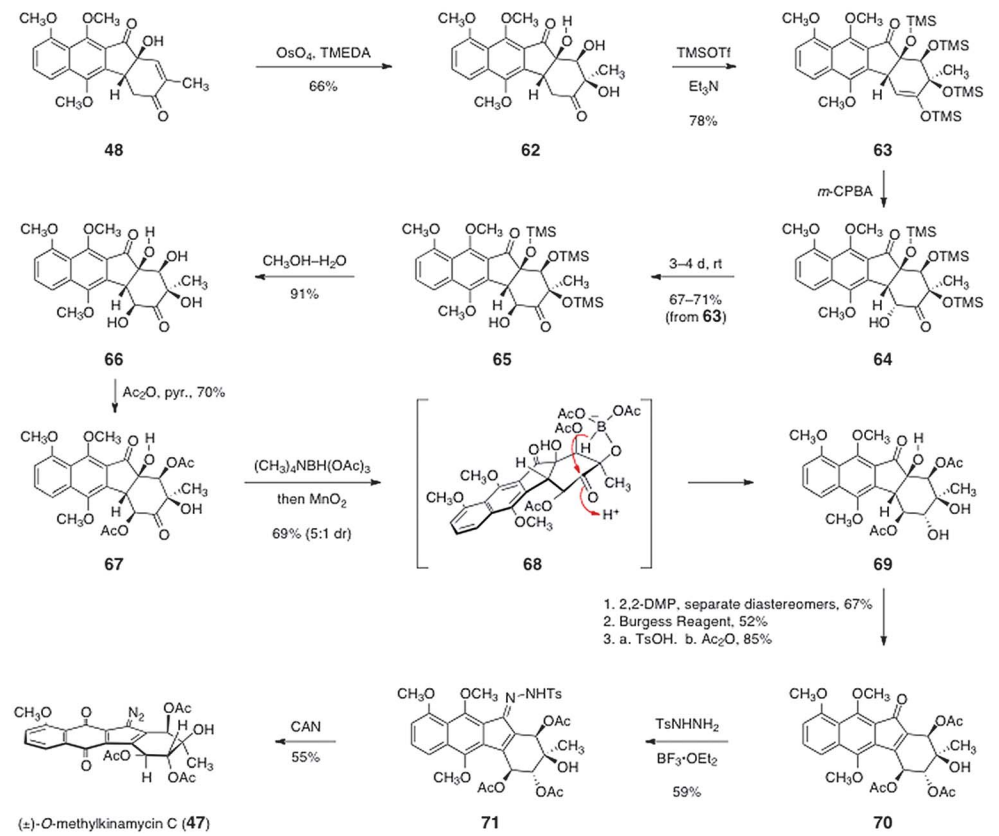

Scheme 10 Completion of the synthesis of (±)-*O*-methylkinamycin C (**47**) by Ishikawa and co-workers.

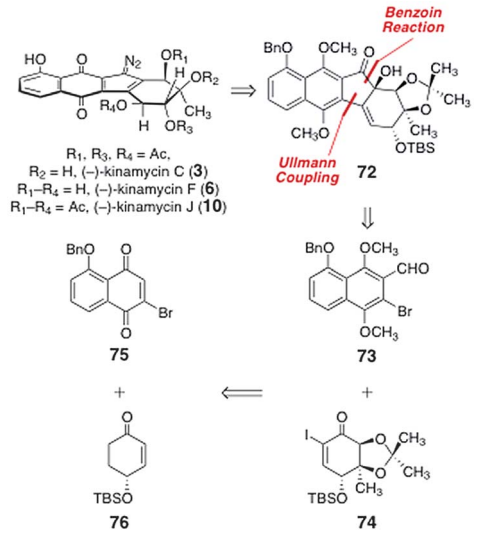

Scheme 11 Retrosyntheses of (−)-kinamycin C (**3**), (−)-kinamycin F (**6**), and (−)-kinamycin J (**10**) by Nicolaou and co-workers.

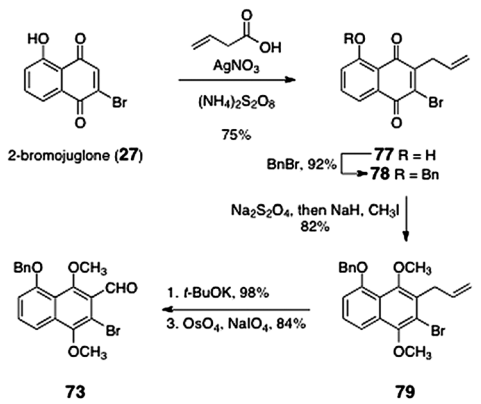

Scheme 12 Synthesis of the *ortho*-bromoaryl aldehyde **73** by Nicolaou and co-workers.

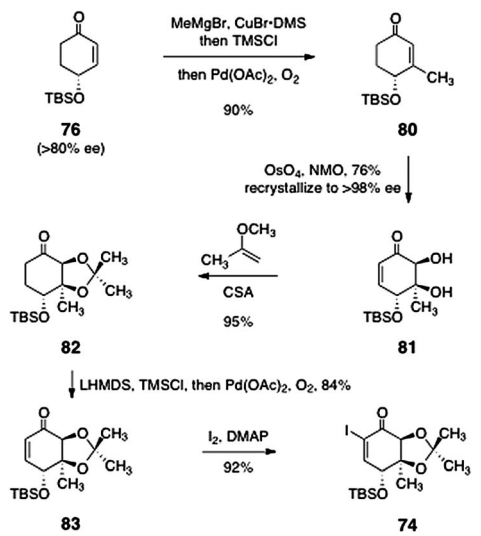

Scheme 13 Nicolaou's synthesis of the α-iodoenone **74**.

The *ortho*-bromoaryl aldehyde **73** was prepared by an efficient five-step sequence (Scheme 12). Beginning with 2-bromojuglone (**27**), radical allylation afforded the allylquinone **77** (75%). *O*-Benzylation formed the benzyl ether **78** (92%). Reduction and *in situ* methylation provided the hydroquinone dimethyl ether **79** (82%). Isomerization of the alkene was effected by treatment of **79** with potassium *tert*-butoxide (98%). The resulting styrene derivative (not shown) was subjected to oxidative cleavage to afford the *ortho*-bromoaryl aldehyde **73** (84%).

Nicolaou's synthesis of the α-iodoenone **74** is shown in Scheme 13. The synthesis began with (*R*)-4-(*tert*-butyldimethylsilyloxy)cyclohex-2-ene-1-one (**76**), prepared in >80% ee by desymmetrization of the corresponding ketone.[51] Copper-catalyzed 1,4-addition of methyl magnesium bromide, trapping with chlorotrimethylsilane, and reoxidation then generated the β-methylcyclohexenone **80** (90%). This product (**80**) was subjected to a diastereoselective catalytic dihydroxylation to afford the diol **81** (76%). The diol **81** was readily recrystallized to >98% ee. Protection of the diol function afforded the acetonide **82** (95%). Generation of the enoxysilane of **82** followed by palladium-mediated oxidation then afforded the enone **83** (84%). Finally, the enone **83** was iodinated under Johnson conditions[52] to provide the target α-iodoenone **74** (92%).

The coupling of the aryl aldehyde **73** and the α-iodoenone **74** was affected by a modified Ullmann reaction (83%, Scheme 14).[53] The resulting arylation product (**84**) was subjected to a benzoin condensation using the triazole catalyst **85**,[54,55] to form the benzoin product **86** (78%). Acylation of the tertiary alcohol function of **86** then afforded the acetate **87** (95%).

The α-acetoxyketone function of **87** was reduced with samarium diiodide,[56,57] to afford the β,γ-unsaturated ketone **88**. Treatment with triethylamine resulted in smooth isomerization of the olefin to form an α,β-unsaturated ketone (not shown). Diastereoselective γ-oxidation (selenium dioxide) generated the secondary alcohol **89** (58%, three steps). The acetonide and silyl ether functions of **89** were cleaved by treatment with hydrofluoric acid to afford a tetraol intermediate (not shown) that was regioselectively acylated at the secondary alcohol functions, providing the triacetate **90** in 89% yield (two steps). Hydrogenolysis of the benzyl ether of **90** followed by silylation of the resulting phenol afforded the key silyl ether **91** (94%). Finally, condensation of **91** with *para*-toluenesulfonylhydrazine afforded a hydrazone (95%, not shown) that was oxidized with ceric ammonium nitrate to form the diazofluorene **92** (42%).

The key diazofluorene **92** was efficiently transformed to (−)-kinamycin C (**3**), (−)-kinamycin F (**6**), and (−)-kinamycin J (**10**, Scheme 15). Cleavage of the silyl ether of **92** (aqueous hydrochloric acid) afforded (−)-kinamycin C (**3**, 95%). Alternatively, treatment of **92** with lithium hydroxide resulted in liberation of the phenol function and saponification of the acetate esters, providing (−)-kinamycin F (**6**) in 92% yield. Finally, acylation of the tertiary hydroxyl of **92** (acetic anhydride, triethylamine), followed by cleavage of the silyl ether (hydrochloric acid), provided (−)-kinamycin J (**10**, 80%, two steps).

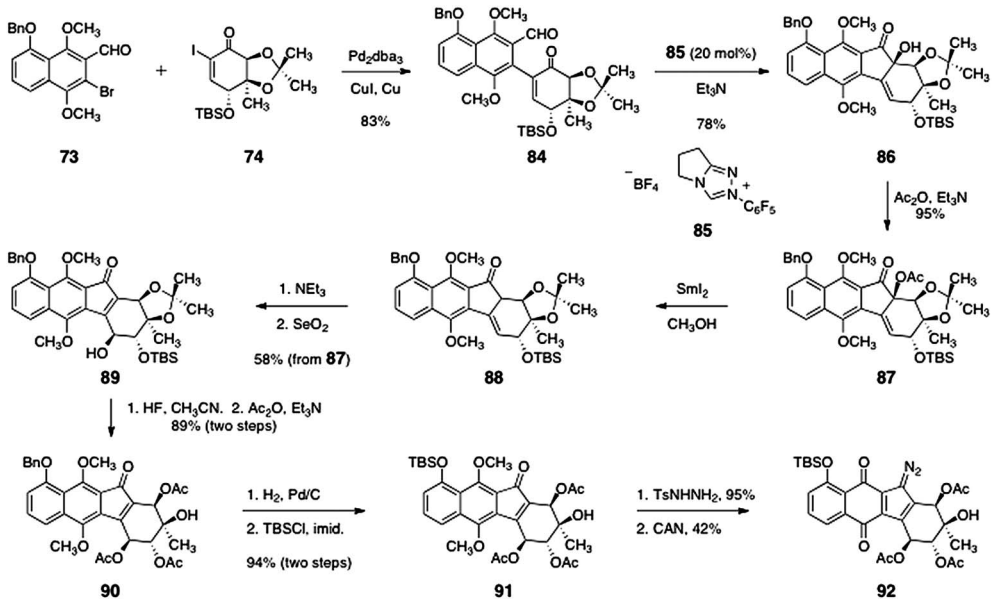

Scheme 14 Nicolaou's synthesis of the penultimate precursor **92**.

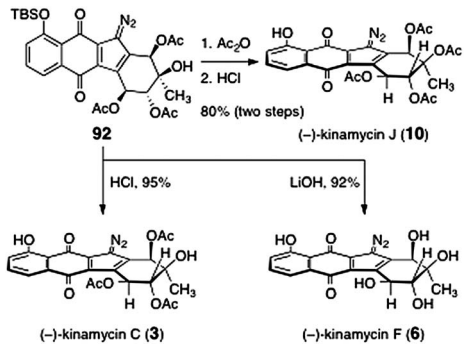

Scheme 15 Completion of the syntheses of (−)-kinamycin C (**3**), (−)-kinamycin F (**6**), and (−)-kinamycin J (**10**) by Nicolaou and co-workers.

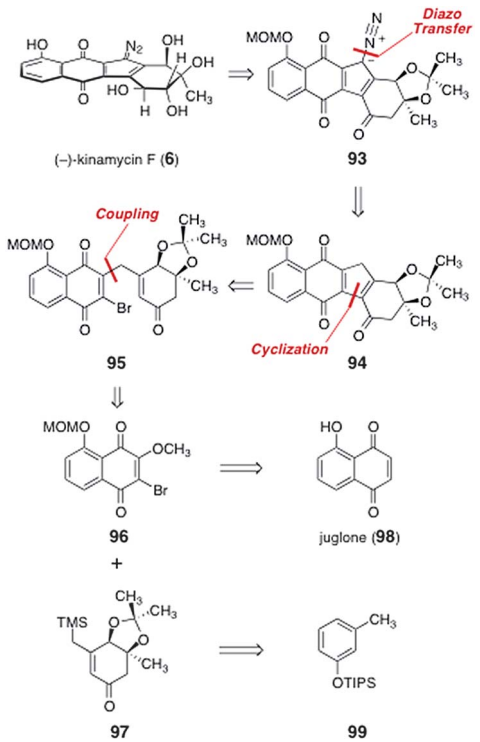

Scheme 16 Retrosynthesis of (−)-kinamycin F (**6**) by Herzon and co-workers.

4.4 Enantioselective synthesis of (−)-kinamycin F (Herzon and co-workers)

In 2010, Herzon and co-workers reported a synthesis of (−)-kinamycin F (**6**).[58] It was envisioned that (−)-kinamycin F (**6**) could be prepared from the protected diazofluorene **93** (Scheme 16). The diazofluorene **93** was formed by diazo transfer to the triacylcyclopentadiene **94** (it was later observed that **94** existed as the hydroxyfulvene tautomer, *vide infra*). The triacylcyclopentadiene **94** was derived from cyclization of the γ-quinonyl enone **95**. Intermediate **95** was synthesized by coupling of *O*-(methoxymethyl)-2-bromo-3-methoxyjuglone (**96**) and the β-trimethylsilylmethyl-α,β-unsaturated ketone **97**. The latter two intermediates were prepared from juglone (**98**) and the silyl ether **99**, respectively.

The synthesis of the *O*-(methoxymethyl)-2-bromo-3-methoxyjuglone (**96**) is shown in Scheme 17. Bromination of juglone (**98**) afforded the dibromojuglone derivative **100**. The phenol function of **100** was protected as its methoxymethyl ether **101** (50%, two steps). Heating mixtures of **101** and sodium carbonate in methanol resulted in regioselective substitution of the C-3 bromide substituent to form *O*-(methoxymethyl)-2-bromo-3-methoxyjuglone (**96**, 96%).

The synthesis of the β-trimethylsilylmethyl-α,β-unsaturated ketone **97** began with the silyl ether **99** (prepared in quantitative yield by silylation of *meta*-cresol, Scheme 18). Birch reduction of **99** formed the cyclohexadiene derivative **102** (>99%). Regio- and

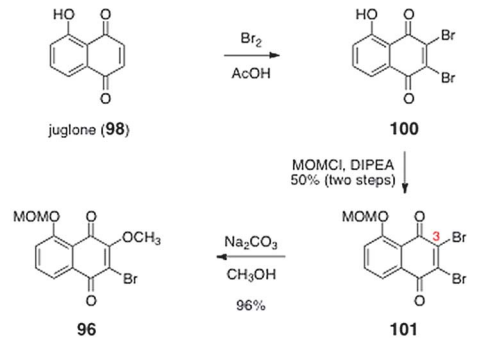

Scheme 17 Synthesis of *O*-(methoxymethyl)-2-bromo-3- methoxy-juglone (**96**).

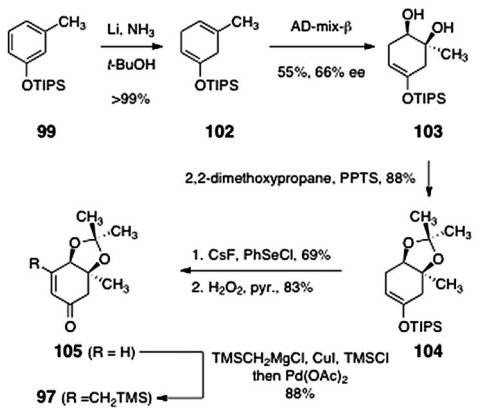

Scheme 18 Synthesis of the β-trimethylsilylmethyl-α, β-unsaturated ketone **97**.

stereoselective dihydroxylation[59] of **102** afforded the diol **103** (55%). The enantiomeric excess of the product was modest (66%), but a subsequent intermediate (**105**) could be recrystallized to >95% ee. The diol **103** was transformed to the acetonide **104** by treatment with 2,2-dimethoxypropane and pyridinium *para*-toluenesulfonate (88%). Next, the enone function was installed by sequential α-selenylation, peroxide oxidation, and elimination (57%, two steps).[60,61] Finally, the unsaturated ketone **105** was homologated by copper-catalyzed 1,4-addition of trimethylsilylmethyl magnesium chloride, trapping with chlorotrimethylsilane, and reoxidation, to afford **97** (88%).

Treatment of a mixture of **96** and **97** with tris(diethylaminosulfonium) trimethyldifluorosilicate [TASF(Et)] resulted in smooth addition–elimination to the naphthoquinone, forming the γ-alkylation product **95** (79%, Scheme 19). Heating of the γ-alkylation product **95** in the presence of palladium acetate, polymer-supported triphenylphosphine, and silver carbonate provided the cyclised product **94** (66%). The product **94** was shown to exist in the hydroxyfulvene tautomer **106**. Treatment of **106** with Hünigs base and trifluoromethanesulfonyl azide[62] resulted in efficient diazo transfer, providing the diazofluorene **93** in 99% yield. Under these conditions, the hydroxyfulvene is deprotonated to generate a cyclopentadienyl anion. Attack of this anion on the triflyl azide reagent provides the observed product (**93**). It is noteworthy that although the anionic charge of the conjugate base of **106** is delocalized over the entire cyclopentadiene ring, only diazotransfer to the desired position generates a stable product. One of the earliest applications of *para*-toluenesulfonyl azide, by von Doering, was in the synthesis of diazocyclopentadiene itself.[63] In the present setting, only the highly electrophilic diazotransfer reagent triflyl azide was found to react with the conjugate base of **106**.

The synthesis of (−)-kinamycin F (**6**) was completed by the pathway shown in Scheme 20. The acetonide protecting group of **93** hinders the approach of reagents from the β-face, and this bias was used to establish the *trans*-1,2-diol function of (−)-kinamycin F (**6**). First, the enoxysilane **107** was formed by treatment with tri-*iso*-propylsilyl trifluoromethanesulfonate and Hünig's base. Addition of dimethyldioxirane resulted in oxygen atom transfer to the α-face of **107** (see **108**), to form a putative silyloxyepoxide intermediate **109**. By employing methanol as co-solvent, **109** was cleaved *in situ* to form the free α-hydroxy ketone **110** (76%). Treatment of **110** with borane–tetrahydrofuran complex at −78 °C, followed by warming to −20 °C, resulted in smooth reduction of the ketone to form the *trans*-1,2-diol **112** (58%). It was proposed that this reduction proceeds *via* the *in situ*-generated borinic ester **111**. Global deprotection (methanol, hydrogen chloride) then afforded (−)-kinamycin F (**6**, 65%).

5 Synthetic studies toward the lomaiviticins

5.1 Introduction

Significant progress toward the syntheses of the lomaiviticins has been achieved, although their complete total synthesis remains

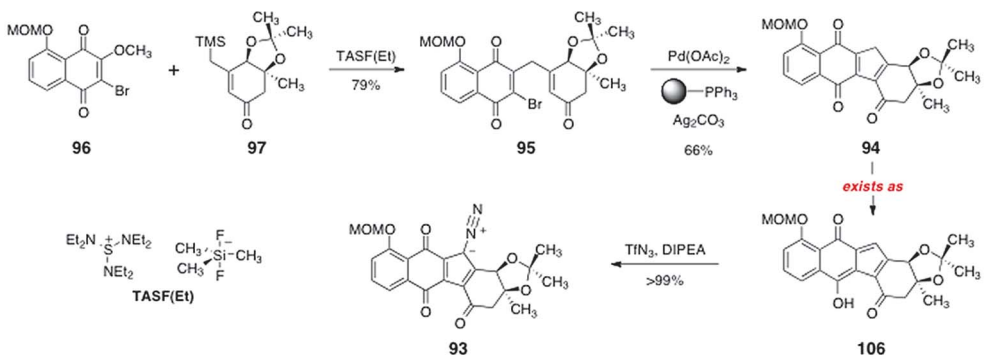

Scheme 19 Synthesis of the diazofluorene **93**.

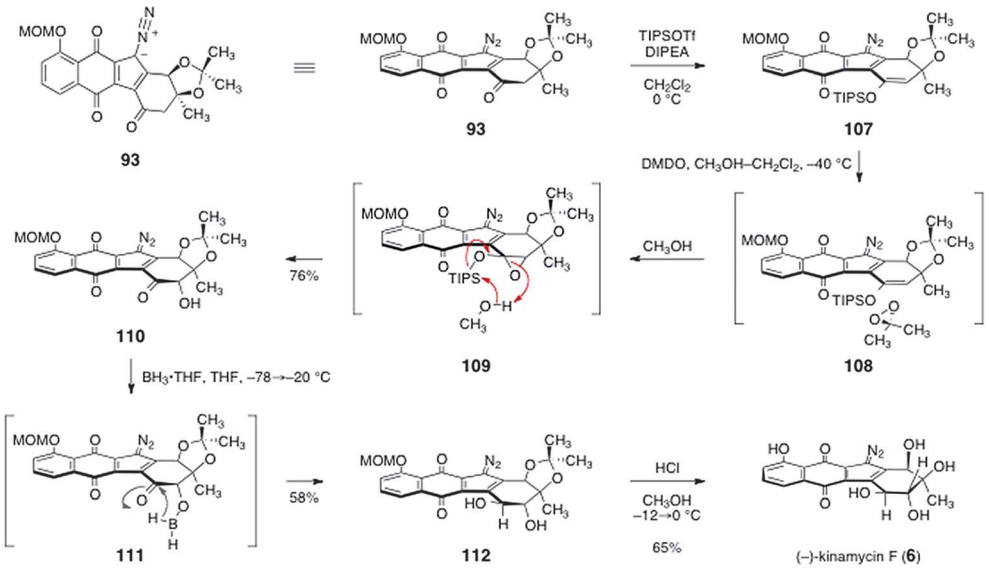

Scheme 20 Completion of the synthesis of (−)-kinamycin F (**6**) by Herzon and co-workers.

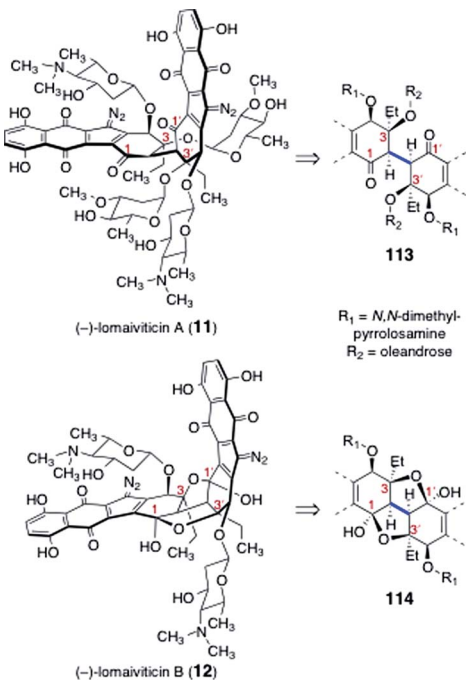

Fig. 3 Lomaiviticins A (**11**) and B (**12**), and their respective dimeric cores (**113**, **114**).

an ongoing challenge. Here we review efforts toward the synthesis of the dimeric core of the lomaiviticins, syntheses of advanced dimeric intermediates, synthesis of the monomeric lomaiviticin aglycon, synthesis of the lomaiviticin aglycon, and finally methods for construction and introduction of the 2,6-dideoxyglycoside residues of the lomaiviticins.

The lomaiviticins contain the densely-functionalized bis (cyclohexene) cores **113** and **114**, respectively (Fig. 3). The syntheses of these substructures present considerable challenges, and was the focus of most early work. At least two significant obstacles are identified. The first involves the stereocontrolled construction of the carbon–carbon bonds (blue in **113** and **114**) that bridge the two halves of each core structure. These bonds are exceedingly hindered (C-3/C-3′ are tetrasubstituted) and the inherent facial selectivity in reactions that might be useful for their construction is ambiguous. The second challenge derives from the substitution about the cyclohexene rings. In the lomaiviticin A core **113**, these rings contain a β-hydroxyketone substructure, which is susceptible to an elimination pathway (see **115** → **116**, Scheme 21). The elimination product **116** can tautomerize to a hydroquinone ether **117**, effectively eliminating all stereocenters in this ring. Somewhat ironically, the steric hindrance that makes formation of the bridging carbon–carbon bond difficult may afford some level of protection against this pathway in late-stage dimeric intermediates. Conversely, monomeric intermediates (*i.e.*, those that lack the bridging C–C bond), which possess much more accessible α-hydrogen atoms, are expected to exhibit heightened reactivity toward this mode of decomposition.

5.2 Syntheses of dimeric core structures (Nicolaou and co-workers)

In order to address the challenges posed by the dimeric core of the lomaiviticins, Nicolaou and co-workers targeted the synthetic constructs **118** and **119** (Scheme 22).[64] It was envisioned that **118** and **119** could be prepared from the tricycle **120**. In their synthetic plan, X is a substituent that may serve to bridge the two

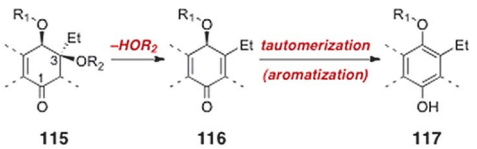

Scheme 21 The β-elimination–aromatization pathway.

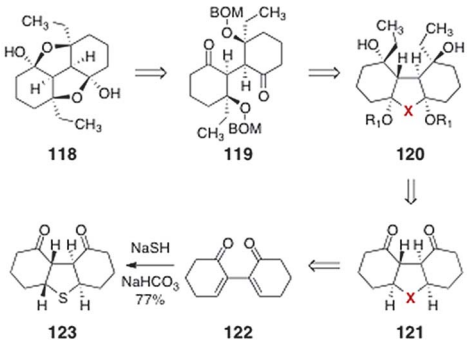

Scheme 22 Retrosynthesis of **118** and **119** by Nicolaou and co-workers.

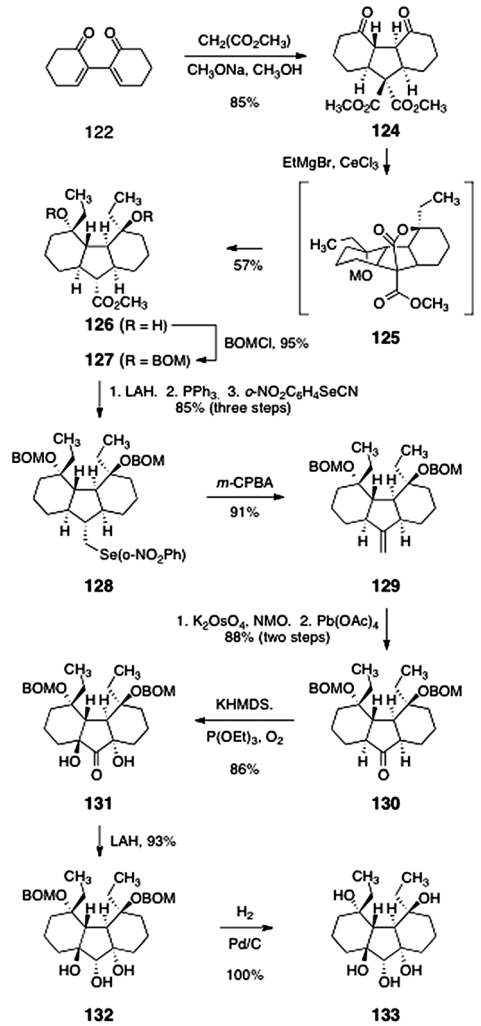

Scheme 23 Synthesis of the tricycle **133** by Nicolaou and co-workers.

rings and, in subsequent transformations, undergo conversion to a dicarbonyl function. The construct **120** was simplified to the diketone **121**. The latter was anticipated to arise from the bis (cyclohexenone) **122**, itself formed by reductive coupling of 2-iodo-cyclohex-2-ene-1-one (not shown).[65]

In preliminary studies, the suitability of a sulfur-based bridge (see **123**) was investigated. Intermediate **123** was formed in a single-step and 77% yield by double 1,4-addition of sodium hydrogen sulfide to **122**. A malonate-based strategy later proved superior; the development of this approach is shown in Scheme 23. Conjugate addition of dimethyl malonate to **122** yielded the double-addition product **124** as a single diastereomer (85%). Treatment of **124** with excess ethyl magnesium bromide in the presence of cerium chloride[66] triggered a cascade reaction, resulting in formation of the product **126** directly (57%). The authors postulated that **126** forms by a sequence comprising addition of the organometal reagent to the ketone functions of **124**, cyclization to form a tetracyclic lactone (**125**), and cleavage of this lactone by an organometal addition–retro-aldol cascade.

Protection of the alcohol functions of **126** as their benzyloxymethyl ethers proceeded smoothly to provide **127** (95%). Reduction of the methyl ester (lithium aluminium hydride) formed a primary alcohol (not shown). Iodination (triphenylphosphine, iodine) and displacement provided the *ortho*-nitrobenzeneselenide **128** (85%, three steps). Selenoxide formation (*m*-CPBA) and *in situ* elimination furnished the alkene **129** (91%). A two-step oxidative cleavage [K_2OsO_4, NMO, then Pb $(OAc)_4$] provided the ketone **130** (88%, two steps). Double α-hydroxylation of the ketone **130** (potassium hexamethyldisilazide, triethylphosphite, dioxygen) furnished the C_2-symmetric diol **131**, as a single diastereomer (86%). Stereoselective reduction of the ketone function (lithium aluminium hydride) yielded the triol **132** (93%). Finally, hydrogenolysis of the benzyloxymethyl ether functions afforded the pentaol **133** (100%).

The completion of the lomaiviticin A core structure **119** is shown in Scheme 24. First, the triol **132** was cleaved (lead tetraacetate) to afford the cyclic hemiacetal **134** (90%). In this transformation, it was postulated that initial oxidation occurs to form a ketoaldehyde (not shown). This intermediate then undergoes spontaneous cyclization to form the observed product (**134**). In the next step, reduction of the latent carbonyl functions of **134** (lithium borohydride) and oxidative cleavage provided the hemiketal **135** (66%, two steps, inconsequential 3 : 1 mixture of diastereomers). The product **135** was then oxidized (TPAP, NMO) to afford the lomaiviticin A core structure **119** (55%).

The synthesis of the lomaiviticin B core **118** is shown in Scheme 25. Oxidation of **133** (lead tetraacetate) produced the monoformate **138** (95%). This transformation was postulated to proceed *via* the **136** and **137**. Deformylation (ammonia,

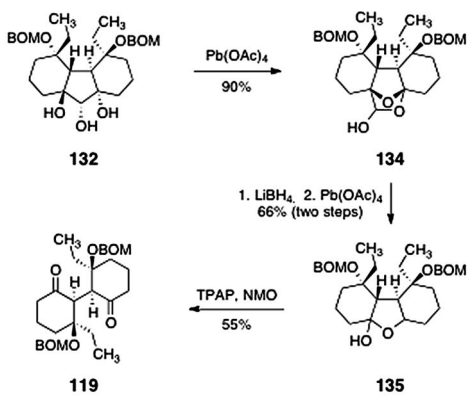

Scheme 24 Completion of the synthesis of the lomaiviticin A core **119** by Nicolaou and co-workers.

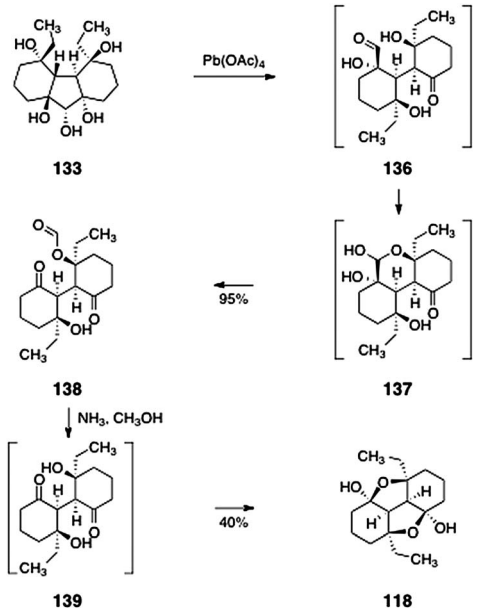

Scheme 25 Completion of the synthesis of the lomaiviticin B core **118** by Nicolaou and co-workers.

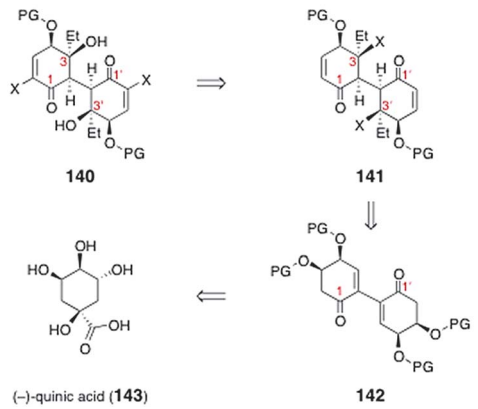

Scheme 26 Retrosynthesis of the lomaiviticin dimeric core **140** by Sulikowski and co-workers.

methanol) then afforded the fused the lomaiviticin B tetracyclic core model system **118** (40%), presumably through the intermediacy of the diketone **139**.

5.3 Synthesis of the C-3/C-3′-dideoxy lomaiviticin core (Sulikowski and co-workers)

Sulikowski and co-workers described an efficient approach to the bis(cyclohexenone) core of lomaiviticin A.[67] The authors targeted the dimeric construct **140** (Scheme 26), which was envisioned to serve as a precursor to the lomaiviticins. The target (**140**) was anticipated to arise from the bis(enone) **141**. The latter in turn could be synthesized by substrate-controlled stereoselective functionalization of **142**. Intermediate **142** was anticipated to derive from (−)-quinic acid (**143**).

Sulikowski's studies began with the cyclohexenone **144** (Scheme 27) prepared from (−)-quinic acid (**143**) by an

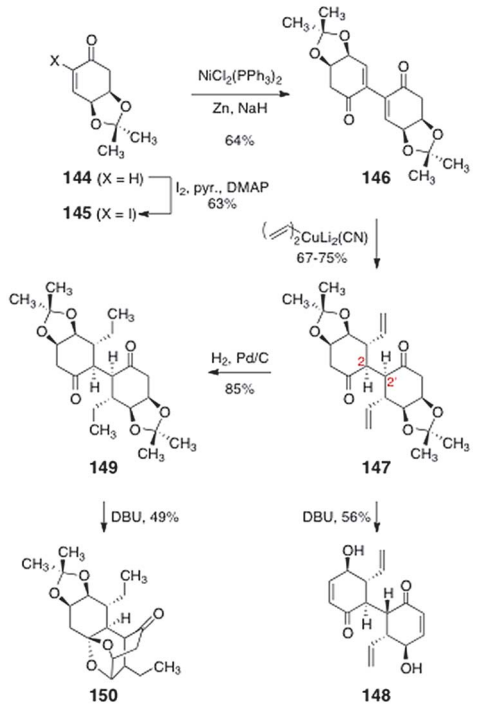

Scheme 27 Studies toward the lomaiviticin core by Sulikowski and co-workers.

established sequence.[68] Iodination[52] then provided the α-iodoenone **145** (63%). Nickel-catalyzed reductive dimerization[65] of the α-iodoenone formed the dimeric product **146** (64%). Double 1,4-addition of vinyl cuprate occurred with complete stereoselectivity, *anti* to the acetonide protecting groups, to form the 1,4-addition product **147** (67–75%). Protonation of the putative enolate intermediates also occurred stereoselectively, establishing the C-2/C-2′ centers of the target. The acetonide functions of **147** could be efficiently cleaved by treatment with DBU. However, under these conditions epimerization of one of the C-2 centers was observed, resulting in isolation of the C_1-symmetric diol **148** (56%). Remarkably, DBU-mediated acetonide cleavage of the reduced product **149** (formed in 85% yield by catalytic hydrogenation of **147**) produced an entirely different outcome. In this case, the bridged ketal **150** was isolated (49%). It is possible that **150** forms by a sequence comprising base-mediated acetonide cleavage, 1,2-addition of the resulting alcohol to the adjacent ketone, and 1,4-addition of the intermediate hemiketal.

In light of these results, the authors examined alternate methods to introduce the ethyl chain and cleave the acetonide function. Toward this end, the allylated bis(enoxysilane) **151** was synthesized by addition of allyltributyltin to **146** in the presence of *tert*-butyldimethylsilyl trifluoromethanesulfonate (97%, Scheme 28). A two-step oxidative cleavage of the alkene functions, followed by reduction (sodium borohydride) formed the diol **152** (75%, three steps). The alcohol functions of **152** were removed by mesylation, displacement with iodide, and catalytic hydrogenation, to afford **153** (55%, three steps). Treatment of **153** with tetrabutylammonium fluoride resulted in cleavage of the enoxysilane and acetonide functions. The

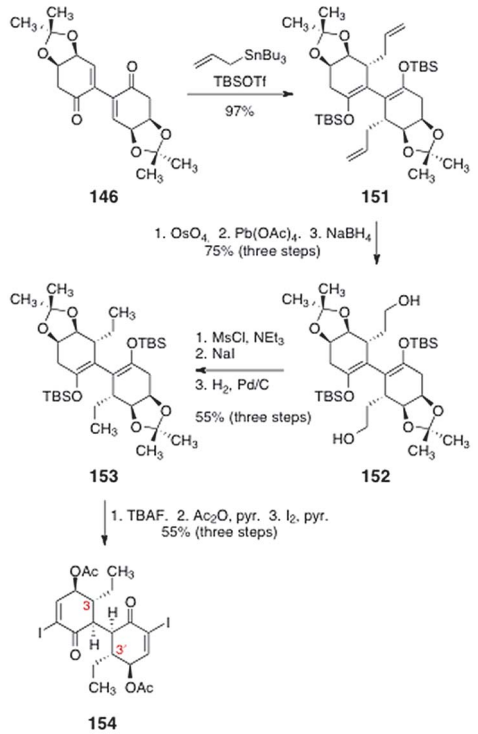

Scheme 28 Synthesis of the C-3/C-3′-dideoxy lomaiviticin core **154** by Sulikowski and co-workers.

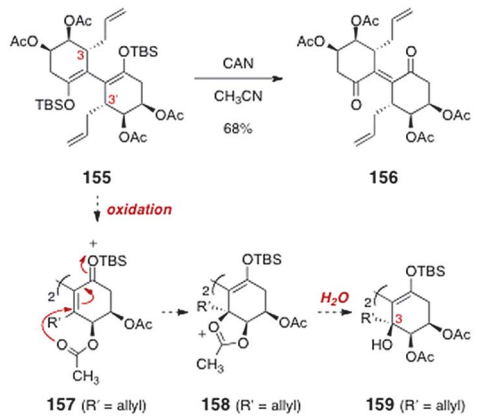

Scheme 29 Attempted formation of the fully oxygenated lomaiviticin core by Sulikowski and co-workers.

resulting enone (not shown) was acylated and then α-iodinated to form the bis(α-iodoenone) **154** (55%, three steps). This construct constitutes the C-3/C-3′-dideoxy core of the lomaiviticins.

Finally, introduction of the C-3/C-3′ hydroxyl substituents was investigated (Scheme 29). The authors envisioned that oxidation of the tetraacetate **155** (itself prepared from **151** in two steps) might form an extended silyloxycarbonium ion (**157**). Intramolecular trapping by the pendant acetate (**158**), followed by hydrolysis, would generate the C-3/C-3′-dioxygenated product **159**. Unfortunately, attempted oxidation of **155** only led to the ene-1,4-dione **156** (68%).

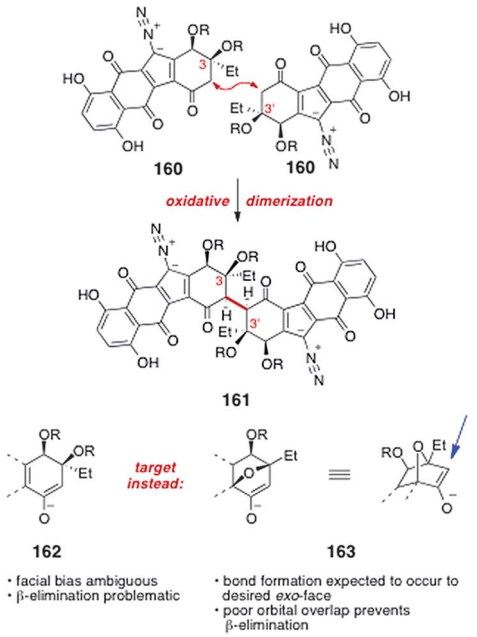

Scheme 30 Oxidative coupling of lomaiviticin monomers **160** and formation of a 7-oxanorbornanone intermediate to circumvent β-elimination and control stereochemistry (Shair and co-workers).

5.4 Synthesis of the complete lomaiviticin carbon skeleton (Shair and co-workers)

Over the period 2008–2010, Shair and co-workers unveiled a strategy for the synthesis of the dimeric core of the lomaiviticins[69] and advanced intermediates containing the entire carbon scaffold of the natural products.[70]

Shair's synthetic approach hinges on the oxidative coupling of monomeric intermediates. As discussed above, although a direct oxidative coupling of two synthetic "lomaiviticin monomers" (2 × **160** → **161**, Scheme 30) is conceptually attractive, in practice such an approach is complicated by issues of stereocontrol and β-elimination (see also Section 5.1). To address these issues, Shair and co-workers targeted intermediates such as **163**, which contain the 7-oxanorbornanone substructure. As a consequence of the fused bicyclic geometry of **163**, carbon–carbon bond formation is expected to occur from the less-hindered, *exo* face (indicated by the blue arrow), providing the stereochemistry required for lomaiviticin synthesis. Moreover, the β-carbon–oxygen antibonding orbital is poorly aligned with the π-system of the enolate **163**. It was therefore expected that β-elimination from this system would be slow.

Initial studies targeted the core system **173** (Scheme 31).[69] Michael addition of the lithium enolate of furanone **165**[71] to oxazolidinone **164**[72] provided the 1,4-addition product **166** in 90% yield (1 : 1 mixture of diastereomers, inconsequential). Acylation of the furanone function generated the acetoxyfuran **167** (92%). An Evans magnesium-catalyzed *anti*-aldol reaction[73] between the acetoxyfuran **167** and β-phenylthioacrolein furnished the *anti*-aldol adduct **168** (60–77%). The aldol adduct **168** was protected as its silyl ether (78%, not shown), and the acetoxy group was cleaved by treatment with potassium cyanide, to afford the furanone **169** (70–95%). Oxidation of **169** (*m*-CPBA)

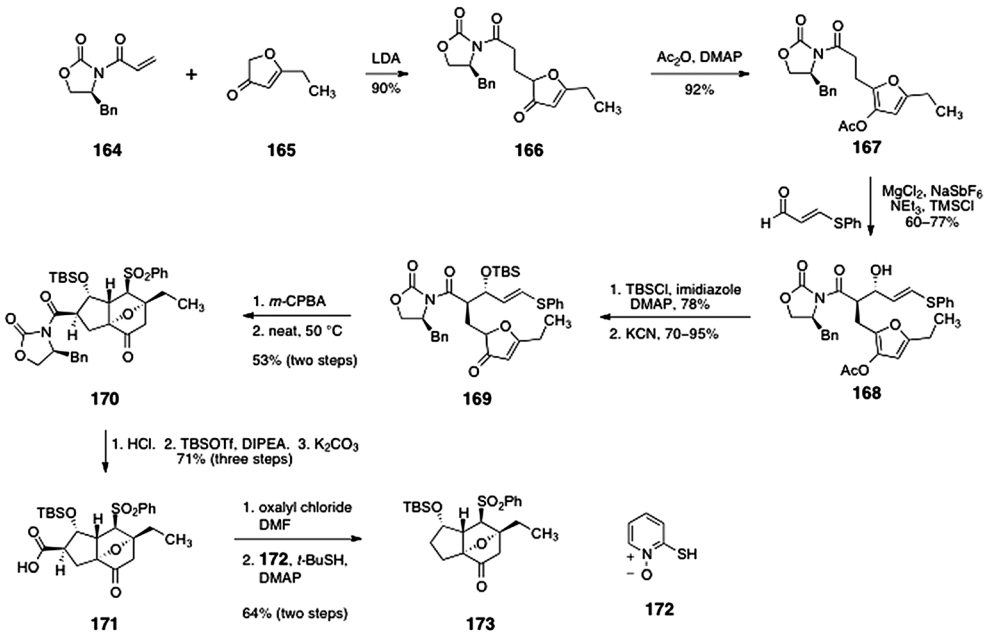

Scheme 31 Synthesis of the tricyclic intermediate **173** by Shair and co-workers.

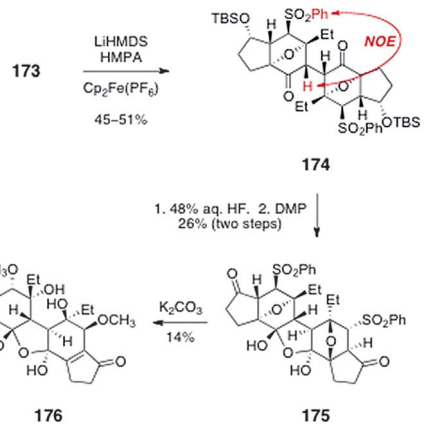

Scheme 32 Dimerization of **173** and elaboration to **176** by Shair and co-workers.

generated a vinyl sulfone (not shown), which upon heating to 50 °C underwent an intramolecular Diels–Alder reaction (potentially *via* the furanol tautomer) to form the *endo*-adduct **170** as the major diastereomer (53%). Acid-mediated cleavage of the imide and silyl substituents, followed by reprotection of the secondary alcohol and saponification of the silyl ester formed the carboxylic acid **171** (71% overall). Barton decarboxylation then provided the target **173** (64%, two steps).

Oxidative dimerization of **173** was realized by enolization with lithium hexamethyl-disilazide followed by addition of ferrocenium hexafluorophosphate (Scheme 32, 45–51%). The stereochemistry of the single C_2-symmetric product that formed (**174**) was established by observation of an NOE between the α-hydrogen and the phenylsulfonyl substituent. The dimer **174** was then desilylated and the resulting alcohols were oxidized with the Dess–Martin periodinane (26%, two steps). Interestingly, the product **175** was shown to incorporate one equivalent of water, to form a stable cyclic hydrate. Finally, the oxanorbornane system of **175** was cleaved by treatment with potassium carbonate in methanol. Under these conditions, the phenylsulfonyl substituent also under went displacement by methoxide to generate the bis(methyl ether) **176** (14%). Attempts to dehydrate **176** to form the core of lomaiviticin B were unsuccessful. The authors postulated that the stability of the hydrate **176** may arise from the vinylogous diketone nature of the system, which is expected to drive the ketone–hydrate equilibrium toward the hydrate form.

The same group extended this strategy to the first synthesis of the lomaiviticin aglycon carbon skeleton.[70] As before, an oxidative dimerization of an oxanorbornanone substrate is the key step in the sequence. These studies began with the norbornanone **170**, which was synthesized by the route shown in Scheme 31. Treatment of **170** with sodium borohydride in allyl alcohol as solvent resulted in diastereoselective reduction of the ketone and cleavage of the imide, to form the allyl ester **177** (89%, Scheme 33). Protection of the secondary alcohol as its pivalate ester (not shown) and cleavage of the silyl ether formed the alcohol **178** (91%, two steps). In the next step, the secondary alcohol was oxidized with dimethylsulfoxide–oxalyl chloride, which formed an α-chloro-β-ketoester (not shown). The chlorine substituent could be readily removed by treatment with zinc in acetic acid to afford the desired β-keto ester **179** in 96% yield (two steps). Treatment of the β-ketoester **179** with bis(triphenylphosphine)-palladium dichloride and tributyltin hydride resulted in decarboxylative deallylation, to provide the ketone **180** (85%). α-Selenation, oxidation, and cheletropic elimination generated the α,β-unsaturated ketone **181** (73%).

In initial studies, the unsaturated ketone was treated with the lithiated cyanophthalide **182**,[74] to afford the annulated product **184** (85%). Protecting group manipulations provided the acetal **186** (66%, two steps).

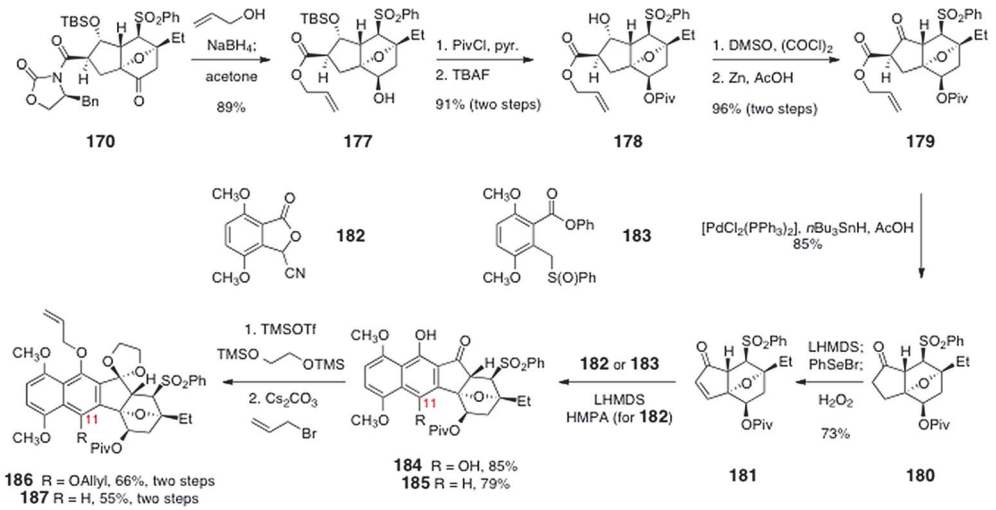

Scheme 33 Elaboration of **170** to the annulated products **186** and **187** by Shair and co-workers.

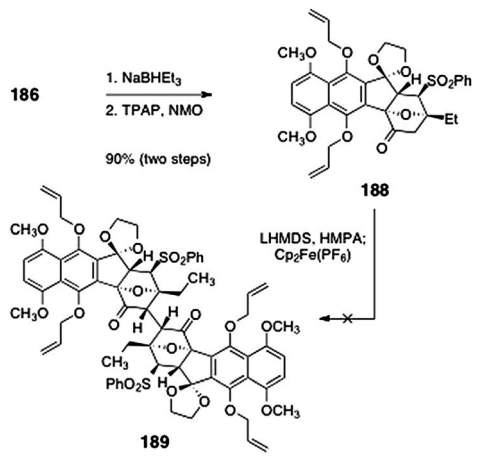

Scheme 34 Attempted dimerization of **188** by Shair and co-workers.

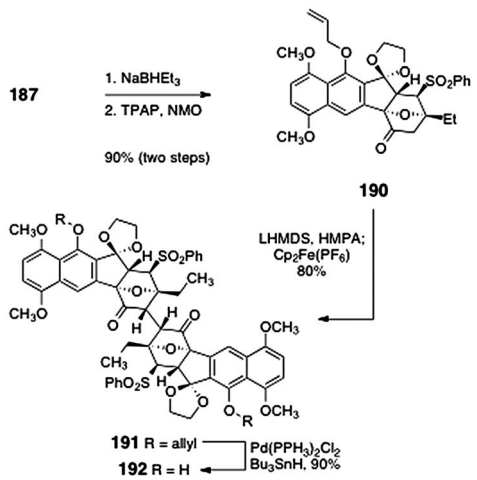

Scheme 35 Successful dimerization of **190** to form the entire lomaiviticin carbon skeleton **191** by Shair and co-workers.

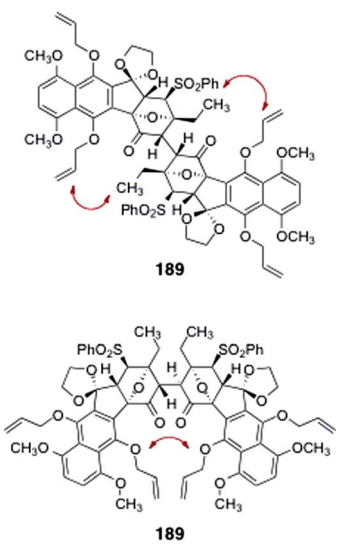

Fig. 4 Steric interactions postulated to prevent the dimerization of **188**.

Sequential pivalate deprotection and oxidation (TPAP, NMO) afforded the oxidative coupling substrate **188** (90%, two steps, Scheme 34). Unfortunately, all attempts to dimerize **188** were unsuccessful. The authors reasoned that the desired product **189** may suffer destabilizing non-bonded interactions, which may inhibit approach of the monomers in the oxidative coupling reaction (Fig. 4).

In order to alleviate these steric interactions, the group pursued the synthesis of **187** (Scheme 33), which lacks the C-11-allyloxy substituent. Hauser annulation[75] of **181** with the sulfoxide **183** provided the C-11-deoxy product **185** (79%). Protecting group manipulations then gave **187** (55%, two steps).

Sequential pivalate reduction and oxidation provided the deoxy dimerization precursor **190** (90%, two steps, Scheme 35). Oxidative dimerization of **190** proceeded in excellent yield to afford the desired C_2-symmetric dimer **191** (80%, 830 mg scale). The allyl ether functions of the dimer **191** could be efficiently cleaved by treatment with bis(triphenylphosphine)palladium dichloride and tri-butyltin hydride (90%). X-ray analysis of the

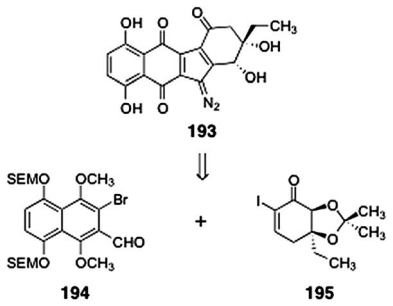

Scheme 36 Retrosynthesis of the monomeric lomaiviticin aglycon **193** by Nicolaou and co-workers.

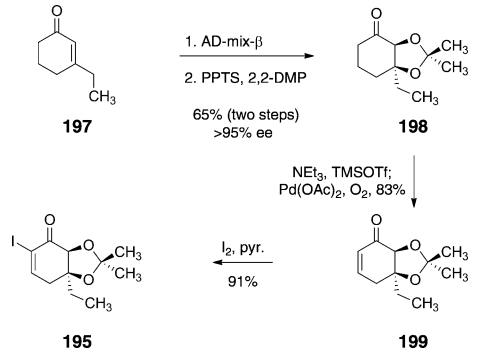

Scheme 38 Synthesis of the α-iodoenone **195** by Nicolaou and co-workers.

product **192** confirmed that it possessed the stereochemistry required for lomaiviticin synthesis. The successful dimerization of **190** compared to **188** highlights the large degree of steric congestion in these molecules and the unexpected consequences of these interactions.

5.5 Synthesis of the monomeric unit of the lomaiviticin aglycon (Nicolaou and co-workers)

Nicolaou and co-workers report the first synthesis of the monomeric unit of the lomaiviticin aglycon (**193**).[76] Retrosynthetically, the target **193** was envisioned to arise from the *ortho*-bromoaryl aldehyde **194** and the α-iodoenone **195** (Scheme 36). The pathway to **193** shares some parallels to the authors' route to (−)-kinamycin C (**3**), (−)-kinamycin F (**6**), and (−)-kinamycin J (**10**),[50] although several modifications were required to accommodate the structural elements of **193**. In the course of these studies, a novel alcohol transposition reaction was discovered.

The *ortho*-bromoaryl aldehyde **194** was prepared from the known intermediate **196** (Scheme 37).[50] Aluminium trichloride-mediated debenzylation (80%), followed by oxidation formed a dimethoxynaphthoquinone intermediate (97%, not shown). Reduction of the quinone and protection of the resulting hydroquinone as its bis(2-trimethylsilylethoxymethyl) (SEM) ether formed the target **194** (92%).

The α-iodoenone **195** was prepared by an efficient four-step sequence (Scheme 38). First, 3-ethyl-cyclohex-2-ene-1-one (**197**) was subjected to a Sharpless asymmetric dihydroxylation reaction, which afforded a *syn*-1,2-diol intermediate (not shown) in 69% yield and >95% ee. Protection of the diol function (pyridinium *para*-toluenesulfonate, 2-methoxypropene) formed the acetonide **198** (94%). Treatment of **198** with trimethylsilyl trifluoromethane-sulfonate and triethylamine formed an enoxysilane (not shown), that was oxidized (palladium acetate, dioxygen) to provide the enone **199** (83%). Iodination[52] of the enone furnished **195** (91%).

The *ortho*-bromoaryl aldehyde **194** and the α-iodoenone **195** were elaborated to the monomeric unit of the lomaiviticin aglycon (**193**) by the sequence outlined in Scheme 39. Palladium-mediated cross-coupling between the **194** and **195** furnished α-arylketone **200** (69%). Benzoin condensation of **200** using the catalyst **85**[55] furnished the α-hydroxyketone **202** (70%), as an inconsequential mixture of diastereomers (3 : 1). Substrates lacking the C-5 substituent gave predominantly the 1,4-addition (Stetter) product in the same transformation. Calculations suggested the bulky C-5 SEM group gears the cross-coupling product toward conformation **201**, *via* a non-bonded interaction with the adjacent methoxy substituent. In the next step, the α-hydroxyketone function of **202** was reduced using samarium diiodide. Bubbling of dioxygen through the reaction mixture, followed by reductive work-up, afforded the γ-hydroxy-α,β-unsatured ketone **203** (76%, 1.5 : 1 inconsequential mixture of diastereomers). It was proposed that this novel transformation proceeds by reductive elimination of the α-hydroxyl function to form an extended samarium enolate. Regioselective addition of dioxygen at the γ-position, and subsequent reduction of the resulting alkyl hydro peroxide intermediate then affords the observed product **203**. Condensation of **203** with *para*-toluenesulfonylhydrazine formed an intermediate hydrazone (91%, not shown). Exhaustive oxidation with the Dess–Martin periodinane (5 equiv.) produced the diazofluorene **204** (62%). Reduction of the quinone function of **204** and acylation of the resulting hydroquinone proceeded smoothly (91%). Deprotection of the acetonide (trimethylsilyl trifluoromethanesulfonate) generated the diol **205** (96%). Finally, oxidative cleavage of the hydroquinone dimethyl ether function (CAN) and saponification of the acetate protecting groups (KOH) furnished the monomeric lomaiviticin aglycon (**193**, 91%, two steps).

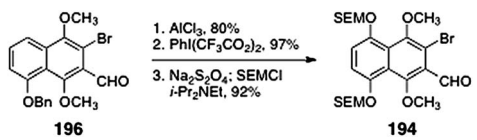

Scheme 37 Synthesis of the *ortho*-bromoaryl aldehyde **194** by Nicolaou and co-workers.

5.6 Synthesis of the lomaiviticin aglycon (Herzon and co-workers)

Herzon and co-workers reported a synthesis of the lomaiviticin aglycon (**206**).[77] The lomaiviticin aglycon (**206**) was prepared from the protected C_2-symmetric dimer **207** (Scheme 40). The latter was synthesized by dimerization of the monomeric diazofluorene **208**.

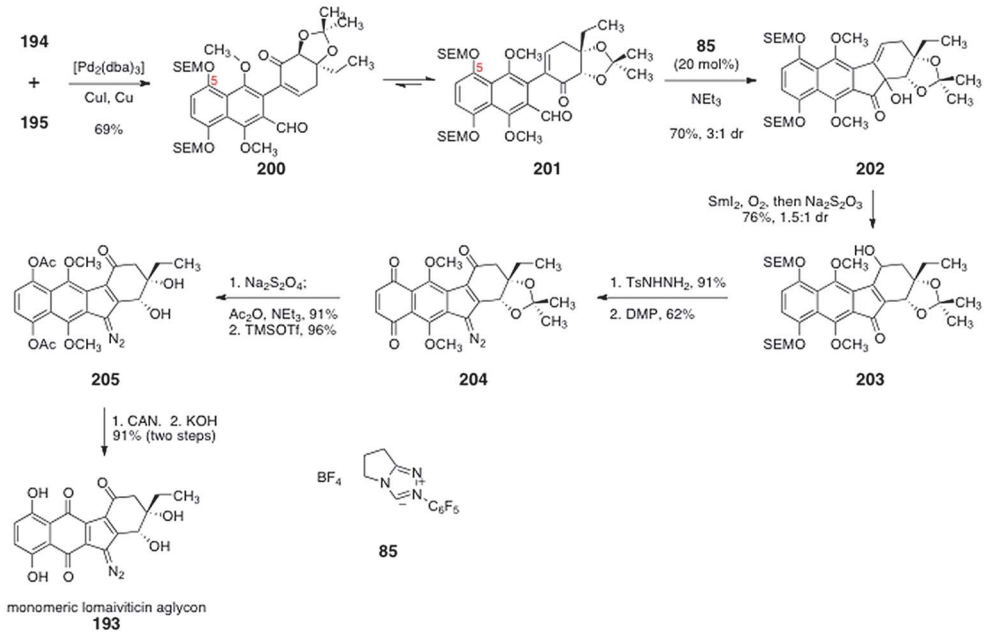

Scheme 39 Synthesis of the monomeric lomaiviticin aglycon **193** by Nicolaou and co-workers.

The monomeric diazofluorene **208** was synthesized by adaptation of the route previously developed for the synthesis of (−)-kinamycin F (**3**).[58] The route to **208** began with silylation of 3-ethylphenol (**209**) to form the silyl ether **210** (>99%, Scheme 41). Birch reduction and asymmetric dihydroxylation then formed the diol **211** (61%, 91% ee). Palladium-mediated oxidation of the enoxysilane of **211** generated the α,β-unsaturated ketone **212** (92%). A mixture of diastereomeric mesityl aldehyde acetals **213** was then formed by heating of **212** in the presence of mesityl aldehyde dimethylacetal and pyridinium *para*-toluenesulfonate (85%, 1 : 1 dr).

Copper-catalyzed addition of trimethylsilylmethylmagnesium chloride, trapping of the resulting enolate with chloro trimethylsilane, and reoxidation then formed the β-(trimethylsilylmethyl)-α,β-unsaturated ketone **214** (82%, 1 : 1 dr). TASF (Et)-mediated coupling of **214** and the dibromonaphthoquinone **215** then formed the γ-quinonylation product **216** (81%). Palladium-mediated cyclization furnished the hydroxyfulvene **217** (95%). Finally, diazo transfer to **217** generated the diazofluorenes **218** and **208** (51% combined yield), which were separated by flash-column chromatography.

In order to dimerize the monomeric diazofluorene **208**, the authors first converted it to the trimethylsilyl enoxysilane **219** (Scheme 42). Treatment of the enoxysilane **219** with a variety of conventional oxidants resulted in aromatization of the substrate (see Scheme 21). Ultimately, the authors found that manganese tris(hexafluoroacetylacetonate) (**220**)[78,79] was effective in promoting the critical dimerization reaction. Thus, treatment of **219** with **220** in benzene at 21 °C formed the desired (2*R*, 2′*R*)-dimer **207** (26–33%), along with the alternate C_2-symmetric dimer **221** (12–23%). The authors found that the orientation of the mesityl protecting group was essential to obtain the desired (2*R*, 2′*R*)-isomer (**207**). Dimerization of the *endo*-mesityldiazofluorene **218** formed the undesired (2*S*, 2′*S*)-dimer exclusively (not shown). It was proposed that the mesityl group of **219** may gear the C-3 ethyl substituent over the over the *Si* face of the enoxysilane, forcing bond formation to occur from the desired *Re* face (Fig. 5).

Deprotection of **207** was effected by treatment with excess trifluoroacetic acid and *tert*-butylhydroperoxide in dichloromethane (39%). The authors determined that the open-chain isomer of the lomaiviticin aglycon (**222**, Fig. 5) was the product that was first formed in the deprotection step. The open-chain isomer **222** was observed to cyclize to lomaiviticin aglycon (**206**) on standing in chloroform-d or upon purification by flash-column chromatography.

6 Syntheses of the lomaiviticin carbohydrates and glycosylation studies

6.1 Introduction

The lomaiviticins contain one or two pairs of 2,6-dideoxyglycosides, β-*N*,*N*-dimethyl-pyrrolosamine (**223**) and α-oleandrose (**224**, Fig. 6). Oleandrose is a relatively common sugar that is found in a number of metabolites, such as the avermectins.[80,81] In contrast, *N*,*N*-dimethyl-pyrrolosamine (**223**) has been found in only one other metabolite, pyrrolosporin.[26,82] While several synthetic routes to both D- and L-oleandrose have been reported,[83–90] *N*,*N*-dimethyl-pyrrolosamine (**223**) had not been synthesized prior to work in the lomaiviticin area.

The oleandrose residue of the lomaiviticins is α-linked. This epimer is both thermodynamically and (typically) kinetically favored in glycosylation reactions. By comparison, the *N*,*N*-dimethyl-pyrrolosamine (**223**) residue is β-linked. The construction of β-linked 2-deoxyglycosides is notoriously difficult and often involves installation of a removable C-2 substituent to control stereochemistry in the glycosylation event.[91] However, these C-2 substituents are most often removed under reducing conditions, which are incompatible with the diazofluorene (*vide infra*). Consequently, the presence of this linkage in the

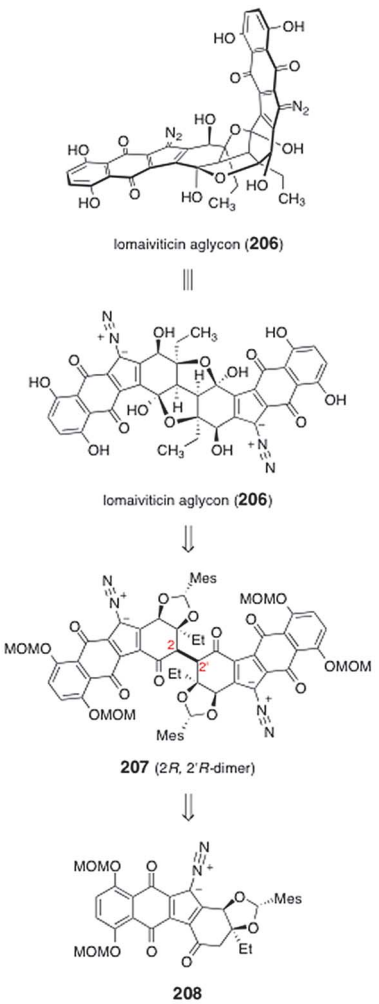

Scheme 40 Retrosynthesis of the lomaiviticin aglycon (**206**) by Herzon and co-workers.

lomaiviticins has inspired new synthetic methods, in particular from the Shair laboratory (*vide infra*).

6.2 Synthesis of the pyrrolosamine residue and the direct formation of β-2-deoxyglycosides by *O*-alkylation (Shair and co-workers)

Shair and co-workers have published two approaches to *N*,*N*-dimethyl-pyrrolosamine (**223**)[92,93] as well as a direct method for the synthesis of β-linked 2-deoxyglycosides by *O*-alkylation. Shair's first approach to **223** begins with the known glycal **225** (Scheme 43).[94] Treatment with trifluoroacetic anhydride followed by displacement of the resulting secondary triflate (not shown) with azide formed the azidoglycal **226** (61%, two steps). The azidoglycal **226** was then hydroacetoxylated to form a glycosyl acetate (81%, not shown). Cleavage of the acetate (dimethylamine) then formed the protected pyrrolosamine derivative **227** as a 4 : 1 mixture of anomers (86%).

In the course of these studies, the authors developed a kinetically-controlled β-selective anomeric *O*-alkylation.[92] Thus, treatment of **227** with allyl bromide and sodium hydride in dioxane at 23 °C formed the β-linked glycoside **228** with excellent selectivity (up to 20 : 1). The authors showed that these conditions were amenable to a range of 2-deoxyglycosides and electrophiles. Although β-selective anomeric *O*-alkylation reactions had previously been reported,[95–98] the studies of Shair and co-workers clearly established that the enhanced β-selectivity arises from destabilizing interactions of the β-anomeric alkoxide with the endocyclic oxygen (rather than from repulsion with the C-2 substituent; see Scheme 44).

The same group also reported a second synthesis of protected pyrrolosamine from L-threonine (**232**, Scheme 45).[93] The starting material **232** was converted to the oxazolidine **233** by treatment with pyridinium *para*-toluenesulfonate and pivaldehyde (71%, 15 : 1 dr). Deprotonation of **233** (lithium di-*iso*-propylamide) followed by treatment with acetic acid afforded the

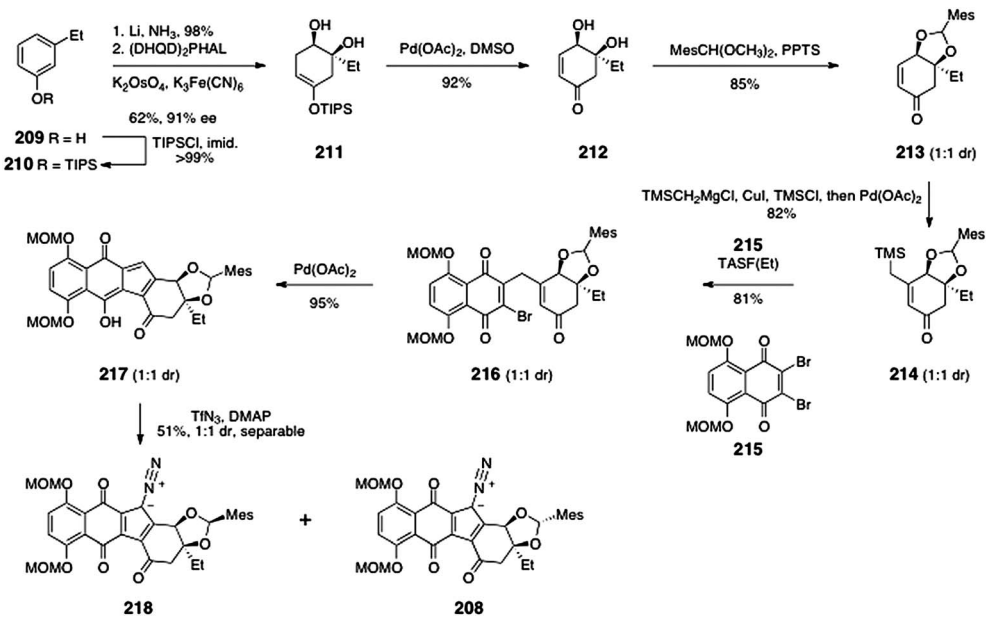

Scheme 41 Synthesis of the diazofluorenes **218** and **208** by Herzon and co-workers.

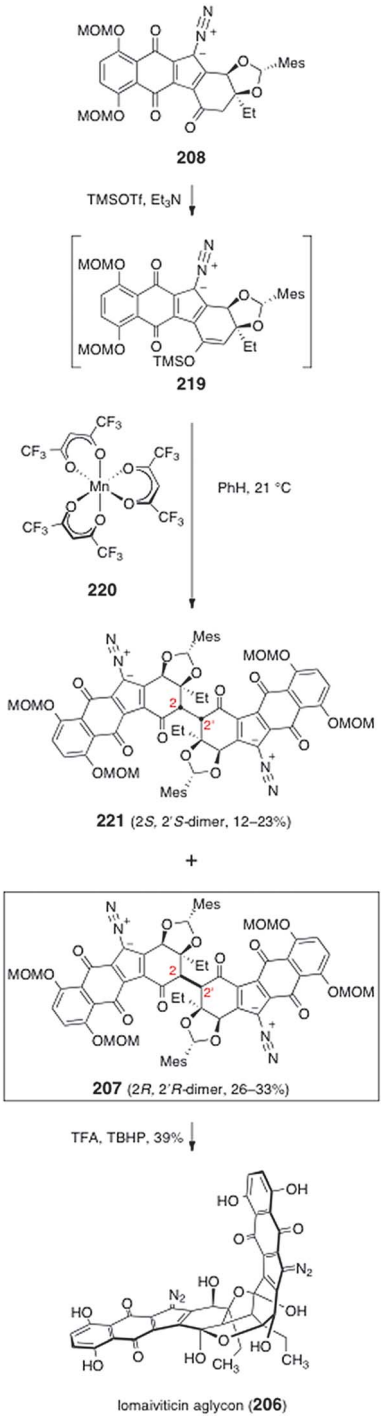

Scheme 42 Conversion of the monomeric diazofluorene **208** to lomaiviticin aglycon (**206**).

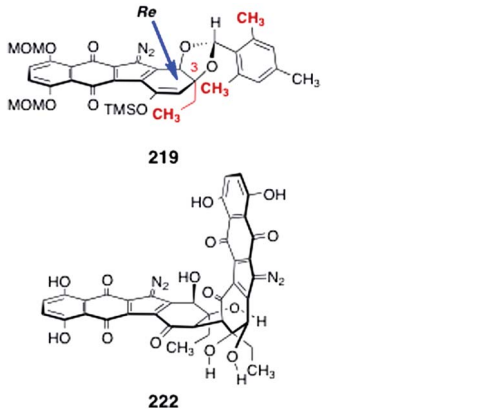

Fig. 5 Stereochemical model for the dimerization of **219** and the structure of the open-chain isomer of lomaiviticin aglycon (**222**).

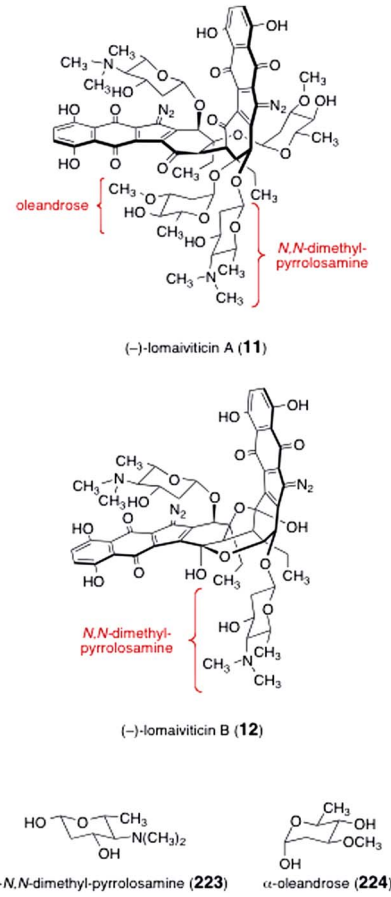

Fig. 6 Structures of lomaiviticins A and B (**11**, **12**, respectively), *N*,*N*-dimethyl pyrrolosamine (**223**), and oleandrose (**224**).

diastereomeric product **234** (>99%). The methyl ester function of **234** was converted to a Weinreb amide (not shown). Reaction of this amide with ethynyl Grignard afforded the alkynyl ketone **235** (68%, two steps). In the next step, diasteroselective reduction provided a propargylic alcohol (not shown) that was protected with tri-*iso*-propylsilyl trifluoromethanesulfonate to yield the silyl ether **236** (88%, two steps). Treatment of **236** with acetic acid cleaved the oxazolidine ring to give the aminoalcohol **237** (58%). Finally, rhodium-catalyzed cycloisomerization provided the glycal **238** (76%), which may be elaborated to *N*,*N*-dimethyl-pyrrolosamine (**223**).

6.3 Synthesis of *N*,*N*-dimethyl-pyrrolosamine and oleandrose. Incorporation into a lomaiviticin model system (Herzon and co-workers)

Herzon and co-workers developed a strategy to synthesize either the D- or L-isomers of the oleandrose and

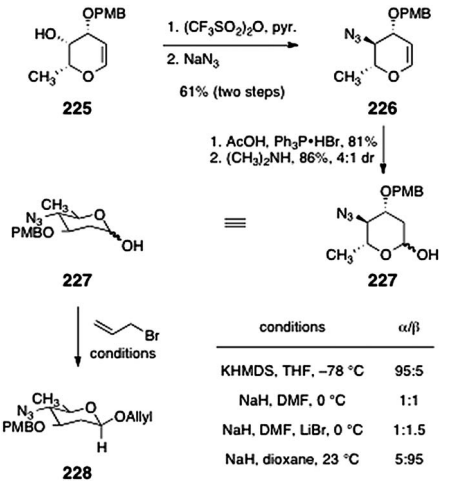

Scheme 43 First-generation synthesis of the protected pyrrolosamine derivative **227** and optimization of the anomeric *O*-alkylation reaction (Shair and co-workers).

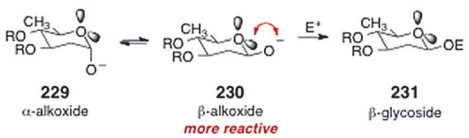

Scheme 44 Lone-pair repulsion model to rationalize the β-selectivity in the anomeric *O*-alkylation reaction (Shair and co-workers).

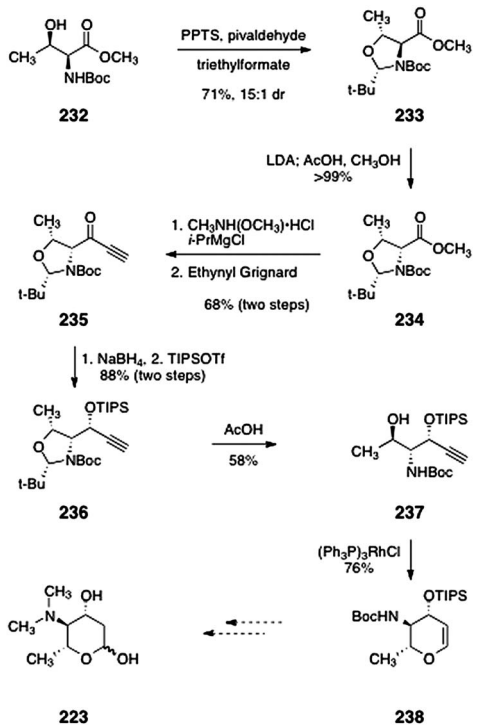

Scheme 45 Synthesis of the glycal **238** (Shair and co-workers).

N,*N*-dimethyl-pyrrolosamine residues of the lomaiviticins.[99] The route to either sugar begins with the known epoxide **239** or its enantiomer ***ent*-239** (Scheme 46), which are available in one step by epoxidation of ethyl sorbate using the Shi catalyst.[100] Heating of the epoxide **239** in the presence of dimethylamine formed the aminoalcohol **240** (51%). Reduction of the ester of **240** (di-*iso*-butylaluminum hydride, −78 °C) afforded the aldehyde **241** (>90%). The aldehyde **241** was then treated with DBU in allyl alcohol as solvent to furnish *O*-allyl-*N*,*N*-dimethyl-D-pyrrolosamine (**242**, 88%). Alternatively, opening of the epoxide ***ent*-239** with allyl alcohol using sulphuric acid as catalyst afforded the alcohol **243** (56%). Reduction of the ester of **243** (di-*iso*-butylaluminum hydride, −78 °C) provided the unsaturated aldehyde **244** (89%). Finally, treatment of the aldehyde **244** with DBU in methanol provided *O*-allyl-L-oleandrose (**245**) as well as its C-3 epimer (not shown) in a 1 : 1 ratio (83%). Resubjection of the C-3 epimer to the reaction conditions served to regenerate the 1 : 1 mixture and increase material throughput.

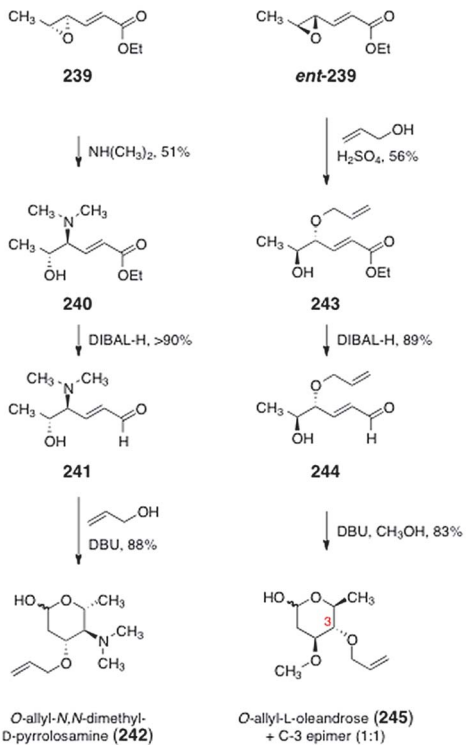

Scheme 46 Synthesis of *O*-allyl-*N*,*N*-dimethyl-D-pyrrolosamine (**242**) and *O*-allyl-L-oleandrose (**245**) by Herzon and co-workers.

With the carbohydrates of the lomaiviticins in hand, Herzon and co-workers studied their regio- and stereoselective incorporation into the model diol **212** (Scheme 47). The authors found that the pyrrolosamine derivative **242** was best activated as its corresponding glycosylphosphinate **246** (47%, α-anomer).[101–103] Treatment of mixtures of the diol **212** and the anomerically-pure α-phosphinate **246** with borontrifluoride etherate furnished a mixture of α- and β-glycosides **248** (57%, α : β = 2 : 3). For the second glycosylation, the protected oleandrose derivative **245** was activated with diethylamino sulfurtrifluoride (DAST, 81%)[104] to afford the glycosyl fluoride **247**. Treatment of β-**248** with the fluoride **247** in the presence of borontrifluoride etherate then formed the bis(glycoside) **249** in 33% yield.

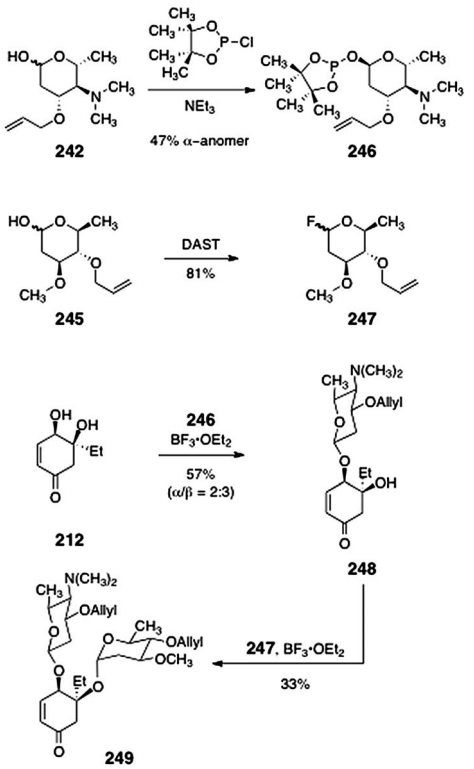

Scheme 47 Synthesis of the lomaiviticin cyclohexenone bis(glycoside) by sequential glycosylation of the diol **212**.

7 Syntheses of metabolites related to the kinamycins and lomaiviticins

7.1 Introduction

A number of kinamycin biosynthetic precursors or shunt metabolites in the biosynthetic pathway have been isolated from the producing strain of the kinamycins. In this section, we present the syntheses of these metabolites.

7.2 Prekinamycin (original and revised structures; Hauser, Echavarren, Birman, and Ishikawa groups)

As discussed in Section 2, prekinamycin (**18**) was isolated from the producing strain of the kinamycins by Gould and co-workers.[8] The structure of prekinamycin was originally proposed to be that depicted as **17** and was subsequently revised to **18** (Fig. 7).

In 1996, Hauser and Zhou reported a synthesis of prekinamycin (**18**, Scheme 48).[105] The authors began with the

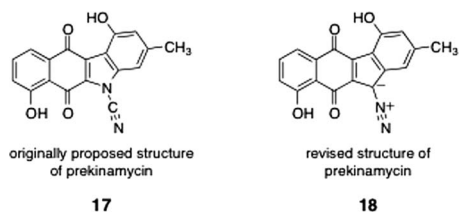

Fig. 7 Originally proposed structure of prekinamycin (**17**) and revised (correct) structure (**18**).

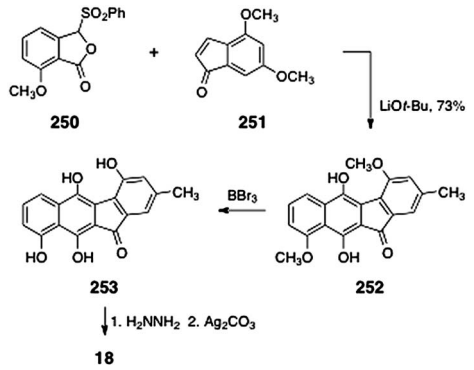

Scheme 48 Synthesis of prekinamycin (**18**) by Hauser and co-workers.

readily-available phthalide sulfone **250** and indenone **251**. Treatment of a mixture of **250** and **251** with lithium *tert*-butoxide resulted in efficient annulation to afford the tetracyclic ketone **252** (73%). The ketone **252** was then demethylated by treatment with boron tribromide. Hydrazone formation (hydrazine) and oxidation (silver carbonate) afforded prekinamycin (**18**, yield not specified). Mal and Hazra utilized Hauser's strategy to synthesize related, but simpler, tetracyclic products.[106]

The cyanocarbazole structure originally proposed for prekinamycin (**17**) was prepared by Echavarren and co-workers.[23] As discussed above, this synthetic work was instrumental in establishing the diazofluorene structure of the kinamycins and lomaiviticins (see Section 2.1). Echavarren's synthesis of **17** began with Stille coupling between the bromojuglone derivative **254** and the arylstannane **255** (99%, Scheme 49). Oxidation with basic *tert*-butyl hydrogen peroxide provided the

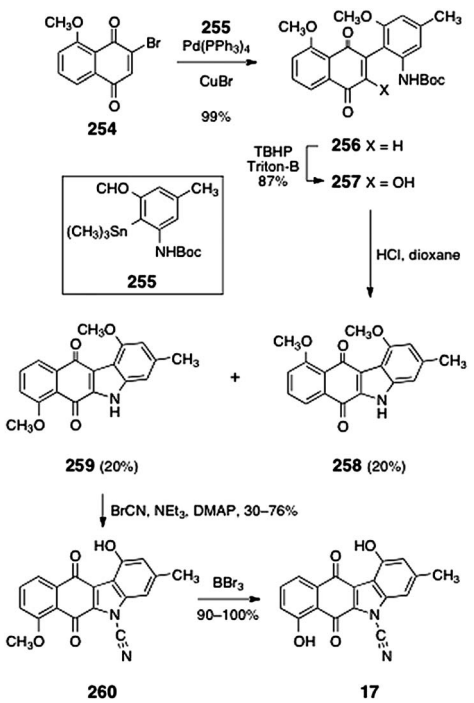

Scheme 49 Synthesis of the originally-proposed structure of prekinamycin (**17**) by Echavarren and co-workers.

hydroxynaphthoquinone **257** (87%). Thermolysis of the hydroxynaphthoquinone **257** induced dehydrative cyclization, forming the expected product **259** (20%) as well as the rearranged product **258** (20%). The desired product **259** was cyanated to form the cyanocarbazole **260** (30–76%) Demethylation (boron tribromide) afforded the originally proposed structure of prekinamycin (**17**, 90–100%).

In 2007, Birman and co-workers reported a highly efficient synthesis of the revised structure of prekinamycin (**18**, Scheme 50).[107] Their synthesis began with base-mediated double acylation of the indanone **262** with the phthalate ester **261** (67–81%). Under these conditions, it was proposed that the dianion of **262** is generated. This dianion undergoes regioselective attack at the more electrophilic ester of the phthalate (see structure **263**). *In situ* Dieckmann condensation then forms the observed tetracyclic product **264**. Condensation of **264** with methanesulfonylhydrazine formed the hydrazone **265** (99%). Demethylation (boron tribromide) afforded the tetraol **266**. Treatment of **266** with triethylamine under an atmosphere of air resulted in spontaneous oxidation to afford prekinamycin (**18**, 85%, two steps).

In 2011, Ishikawa and coworkers reported a synthesis of prekinamycin (**18**, Scheme 51).[108] Their synthesis began with a Suzuki coupling between the aryl boronic acid **267** and the bromide **268**[108] (97%). Oxidation of the coupling product **269** with basic hydrogen peroxide formed the carboxylic acid **270** (80%). Conversion to the acyl chloride (oxalyl chloride) and intramolecular Friedel–Crafts reaction gave the tetracyclic ketone **271** (81%, two steps). Cleavage of the methoxymethyl and methyl protecting groups (boron tribromide) then provided the tetraol **272**. Treatment of the unpurified tetraol with *para*-toluenesulfonylhydrazine and oxidation with silver carbonate then afforded prekinamycin (**18**, 47%, three steps).

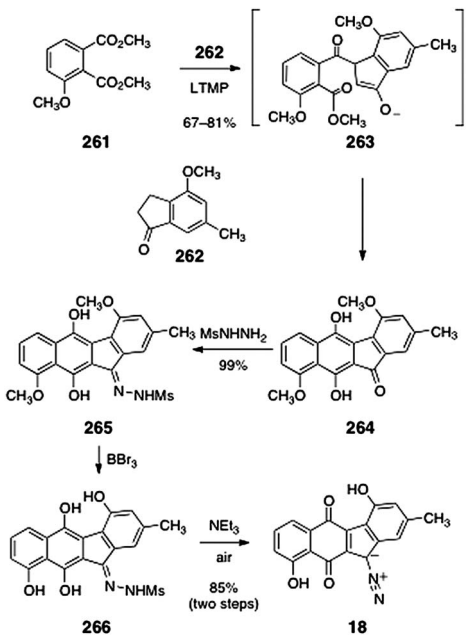

Scheme 50 Synthesis of prekinamycin (**18**) by Birman and co-workers.

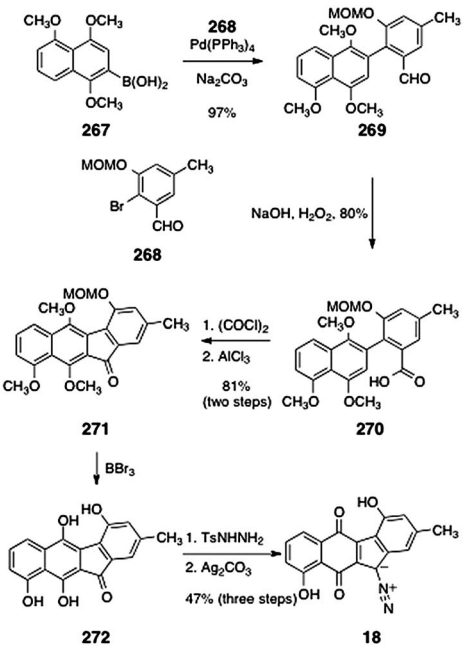

Scheme 51 Synthesis of prekinamycin (**18**) by Ishikawa and co-workers.

7.3 Isoprekinamycin (Dmitrienko and co-workers)

Dmitrienko and co-workers reported the total synthesis of isoprekinamycin (**281**, Scheme 52),[109] a diazobenzo[*a*]fluorene natural product that was isolated from the producing strain of the kinamycins.[8,110] The synthesis began with the readily-available alcohol **273**, which was converted to the nitrile **274** by a two-step sequence (69%). Palladium-mediated borylation afforded the arylboronate ester **275** (82%). Suzuki coupling of the arylboronate ester **275** with the bromoindenone **276** afforded the α-arylketone **277** (85%). The α-arylketone **277** was reduced with a mixture of *n*-butyllithium and di-*iso*-butylaluminumhydride,[111] to form the putative aluminium alkoxide intermediate **278**. Addition of lithium di-*iso*-propylamide to the reaction mixture promoted cyclization to afford the tetracycle **279**. The tetracycle **279** was then *O*-methylated (potassium carbonate, methyl iodide) and the nitrile function was hydrolyzed (hydrogen peroxide, potassium carbonate, methyl sulfoxide). Under these conditions, the secondary alcohol was also oxidized, providing the amidoketone **280** in 51% yield from **277**. Finally, Hoffmann rearrangement, cleavage of the resulting carbamate, diazotization, and demethylation, afforded isoprekinamycin (**281**, 46%, four steps).

7.4 Kinobscurinone (Snieckus and co-workers)

A formal total synthesis of kinobscurinone (**21**, Scheme 3) was reported by Snieckus and co-workers.[112] Their synthesis began with Suzuki coupling of the aryl bromide **282** and the boronic acid **283** (95%, Scheme 53). The coupling product **284** was then treated with excess *s*-butyllithium to generate an *ortho*-metalated aryl carbamate (not shown). Trapping with chlorotrimethylsilane formed the aryl silane **285** (97%). Treatment of **285** with excess lithium di-*iso*-propylamide induced arene metalation–carbamoyl transfer to form the aryl amide **286** (62%).

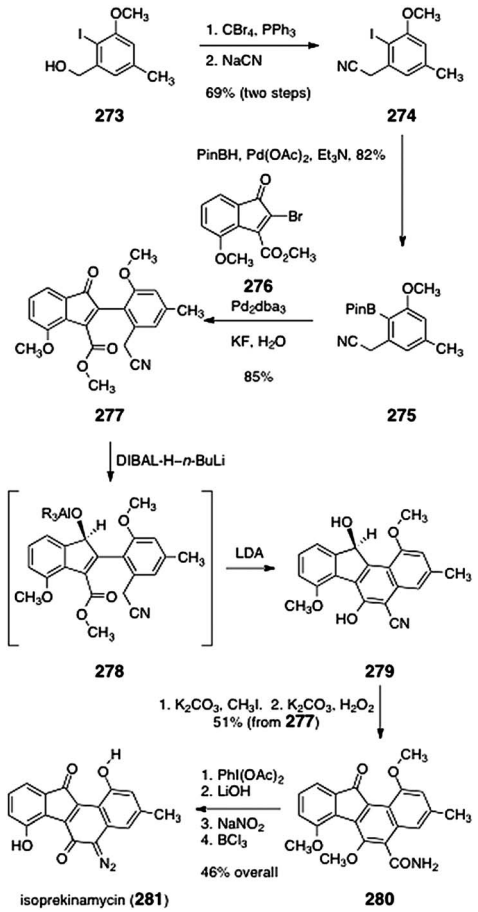

Scheme 52 Synthesis of isoprekinamycin (**281**) by Dmitrienko and co-workers.

Methylation of **286** formed the tetramethyl ether **287** (96%). Treatment of **287** with excess lithium di-*iso*-propylamide generated the tetracycle **288** (78%). Protodesilylation (trifluoroacetic acid, reflux) produced tetramethylkinobscurinone (**289**, quant.). Tetramethylkinobscurinone (**289**) had previously been transformed to kinobscurinone (**21**) by Gould and co-workers.[27]

7.5 Stealthins (Gould and Kamikawa groups)

Stealthins A–C (**290**, **291**, and **22**, respectively, Fig. 8) were isolated from the fermentation broth of various strains of *Streptomyces*.[28,113] Owing to the presence of a stable free radical valence tautomer, these metabolites are NMR-silent and exhibit potent radical scavenging activity.

Gould reported the synthesis of stealthin C (**22**) from tetramethylkinobscurinone (**289**, Scheme 54).[28] Treatment of tetramethylkinobscurinone (**289**) with hydroxylamine formed the oxime **292** (99%). Cleavage of the methyl ethers afforded the quinone **293** (69%). Finally, dithionite reduction provided stealthin C (**22**, 80%).

Kamikawa and Koyama reported the synthesis of stealthin C dimethyl ether (**301**, Scheme 55).[114] The synthesis began with a Suzuki coupling of the arylboronic acid **294** and the aryl bromide **295** (100%). Oxidation of the aldehyde function of the coupling product **296** afforded the carboxylic acid **297** (91%).

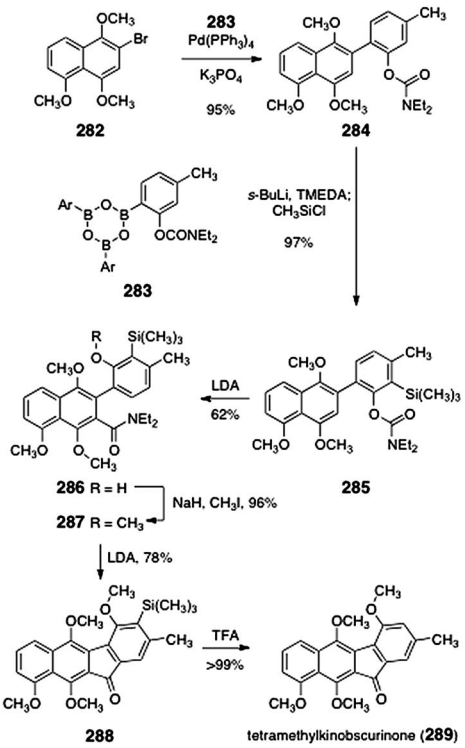

Scheme 53 Synthesis of tetramethylkinobscurinone (**289**) by Snieckus and co-workers.

Activation of the carboxylic acid (oxalyl chloride) formed an acid chloride (not shown), that on treatment with titanium chloride underwent efficient Friedel–Crafts ring closure, to afford the tetracyclic ketone **298** (79%). Condensation of **298** with *O*-benzyl hydroxylamine generated an oxime ether (77%, not shown). Oxidative demethylation using ceric ammonium nitrate and pyridine 2,6-dicarboxylic acid *N*-oxide (**299**) afforded the naphthoquinone **300** (77%). Finally, reduction of **300** (zinc, acetic acid) afforded stealthin C dimethyl ether (**301**, 80%).

8 Chemical biological studies

8.1 Introduction

The kinamycins and lomaiviticins are potent anticancer and antimicrobial agents. (−)-Kinamycin C (**3**) exhibited a $<GI_{50}>$ = 340 nM against the NCI 60 cell line panel.[14] (−)-Lomaiviticin A (**11**) exhibited IC_{50} values in the low nanomolar range, with activities as low as 10 pM against ovarian cell lines.[12] Moreover, the toxicity profiles of **3** and **11** are unique, which is indicative of a novel mechanism of action. Various kinamycins and

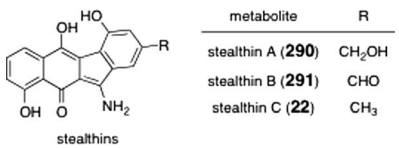

Fig. 8 Structures of the stealthins A, B, and C (**290**, **291**, and **22**, respectively).

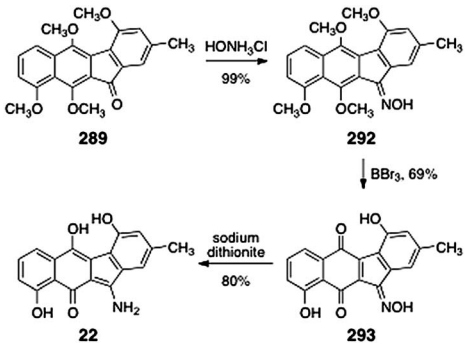

Scheme 54 Synthesis of stealthin C (**22**) from tetramethylkinobscurinone (**289**) by Gould and co-workers.

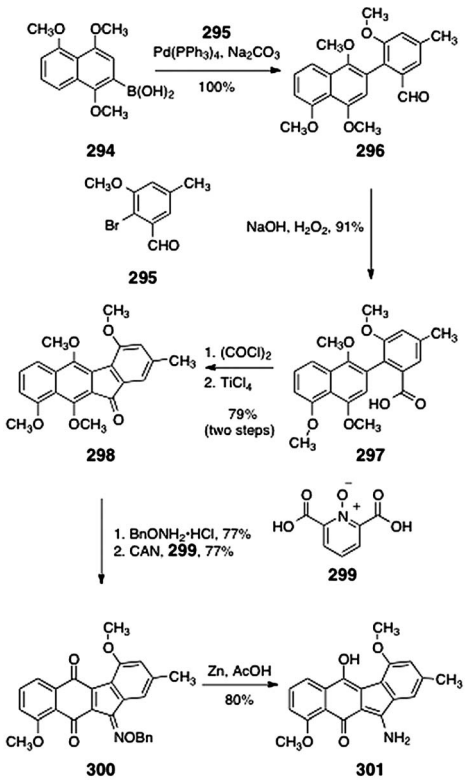

Scheme 55 Synthesis of stealthin C dimethyl ether (**301**) by Kamikawa and Koyama.

lomaiviticins also inhibit the growth of Gram-positive and Gram-negative bacteria at low micromolar–nanomolar concentrations.[12]

Diazo and diazonium-based DNA cleaving agents, and their mode of action, have been reviewed.[18] Herein, we will discuss studies that relate directly to the kinamycins and lomaiviticins.

8.2 Chemical biological studies of the kinamycins and lomaiviticins (Melander, Hasinoff, and Dimitrienko groups)

Melander and co-workers have shown that the kinamycins cleave dsDNA in the presence of a reducing co-factor.[115,116] This dsDNA cleavage appears to be non-sequence specific, suggesting a free radical mechanism may be operative. Experiments employed dithiothrietol (DTT) or glutathione (GSH) at intracellularly-relevant concentrations. The authors speculated that reduction of the quinone to form a hydroquinone, such as **302**, may occur (Scheme 56). Reduction of the quinone may trigger loss of the diazo function to form a reactive *ortho*-quinone methide (**303**). Alternatively, the hydroquinone **302** may form an adduct with an exogenous nucleophile (see structure **304**). The adduct (**304**) may undergo decomposition to form alkyl-centered radicals, which would be expected to damage DNA. These hypotheses are similar to those put forth independently by the Hasinoff–Dimitrienko and Feldman research groups (*vide infra*). It is quite possible that the observed cytotoxic effects of the kinamycins arise from a combination of these reaction pathways.

The Melander group has also shown that simple diazofluorenes, such as **306** and **307**, are able to cleave dsDNA,[117] suggesting the diazofluorene as a general DNA-cleaving functional group. The substitution pattern about the diazofluorenes had a measurable effect on their cleavage ability. 1-Methoxydiazofluorene (**306**) exhibited DNA cleaving abilities similar to kinamycin D (**4**), whereas 4-aminodiazofluorene (**307**) was found to cleave DNA even in the absence of a reducing agent.

Hasinoff and Dmitrienko have suggested that the cytotoxicity of the kinamycins may be due to generation of reactive oxygen species (ROS) *in vivo*.[118] Consistent with Melander's studies, these authors observed reaction between kinamycin F (**6**) and GSH. Electron paramagnetic resonance studies showed that the

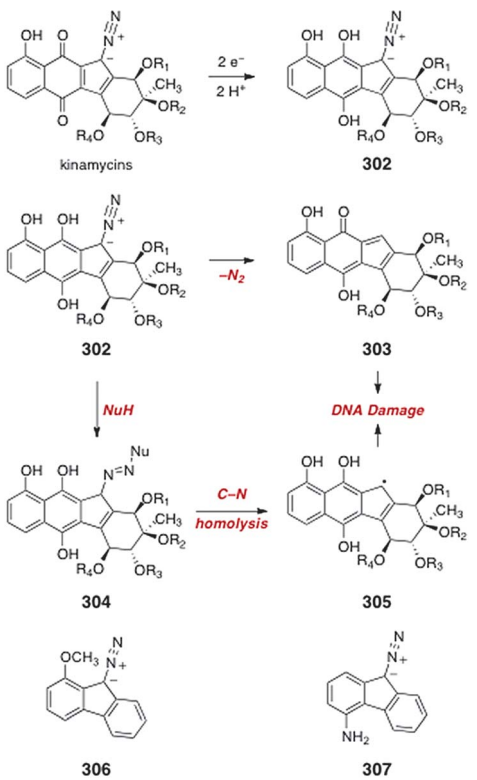

Scheme 56 Proposed reaction pathways for the kinamycins under reducing conditions (Melander and co-workers).

reaction of kinamycin F (**6**) with GSH formed a semiquinone free radical. By modulating the intracellular concentration of GSH, the authors were able to show that the toxicity of kinamycin F (**6**) correlated linearly with [GSH], implicating this reaction pathway in the cytotoxic effects of kinamycin F (**6**). The reagent 2-oxo-4-thiazolidinecarboxylic acid was used to increase cellular GSH levels in K562 cells. Buthionine sulfoximine was used to decrease GSH levels in the same cell line. The authors also showed that kinamycin F (**6**) weakly bound DNA. Using an ethidium bromide displacement assay, the authors determined K_{app} to be 9 $\times$ 10^4 M^{-1}. This is *ca.* 300-fold weaker than doxorubicin. *In vitro* studies revealed that kinamycin F (**6**) induced small amounts of DNA cleavage in the absence of a reducing co-factor. In the presence of GSH, kinamycin F (**6**) efficiently cleaved DNA. This cleavage activity decreased on addition of deferoxamine, dimethyl sulfoxide, and catalase, suggesting DNA damage occurs in an iron-, hydrogen peroxide-, and hydroxyl radical-dependent fashion.

Additional studies using synchronized K562 cells showed an accumulation of cells in the S phase, and delayed entry into the G_2/M phase on treatment with kinamycin F (**6**).[118] Kinamycin F (**6**) activated the caspase-3/7 pathway, leading to an increase in apoptosis. The authors show that the production of cyclin D3 was diminished in cells treated with kinamycin F (**6**), although the protein itself was stable in the presence of **6**. It was shown that **6** decreased the level of cyclin D3 mRNA, but had little interaction with the DNA or mRNA itself. In light of the poor DNA and mRNA binding and high concentrations of kinamycins required for DNA damage, the authors speculated that the kinamycins may target a protein in the cyclin D3 production pathway.

Little is known about the mechanism of action of the lomaiviticins, most likely due to difficulties associated with their fermentation. In the isolation report, lomaiviticin A (**11**) was reported to cleave dsDNA under reducing conditions.[12] Further studies are required to fully evaluate this reactivity.

8.3 *In vitro* reactivity studies (Jebaratnam, Dmitrienko, Feldman, Skibo, and Moore groups)

The *in vitro* and tissue culture reactivity of simple diazofluorenes has been studied by several groups. In 1995, Arya and Jebaratnam reported that DNA was efficiently cleaved when incubated in the presence of the diazofluorene **308** and cupric acetate (Scheme 57).[119] Control experiments indicated that both reagents were required for cleavage. The authors proposed that the diazofluorene **308** may undergo oxidation to the free radical **309** and that the latter might be the active DNA-cleaving agent. It was suggested that the quinone function of the kinamycins may

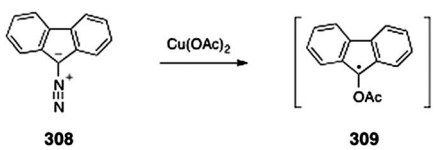

Scheme 57 Proposed oxidation of **308** to form a reactive free radical intermediate (Arya and Jebaratnam).

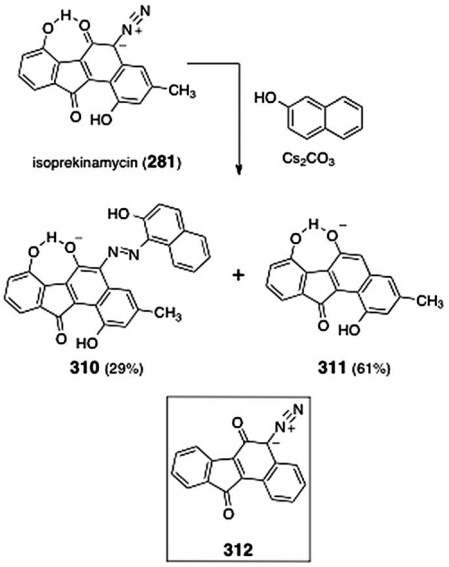

Scheme 58 Reaction of isoprekinamycin (**281**) with β-naphthol under basic conditions (Dmitrienko and co-workers).

act as an internal oxidant toward the diazo group, triggering the formation of a radical similar to **309**. However, other studies seem to suggest that the kinamycins and lomaiviticins are reductively activated.

Dmitrienko and co-workers studied the *in vitro* reactivity of isoprekinamycin (**281**, Scheme 58).[120] It was shown that isoprekinamycin (**281**) underwent addition of β-napthol to form the alkylation product **310** (29%), as well as the reduced product **311** (61%). The authors proposed that a hydrogen-bonding interaction between the quinone and the adjacent phenol (see structure **281**) may increase the electrophilicity of the α-diazoketone function of isoprekinamycin (**281**). The related synthetic intermediate **312**, which lacks this interaction, was unreactive under otherwise identical conditions. The authors suggested that the kinamycins and lomaiviticins may exert their cytotoxic effects by undergoing addition of

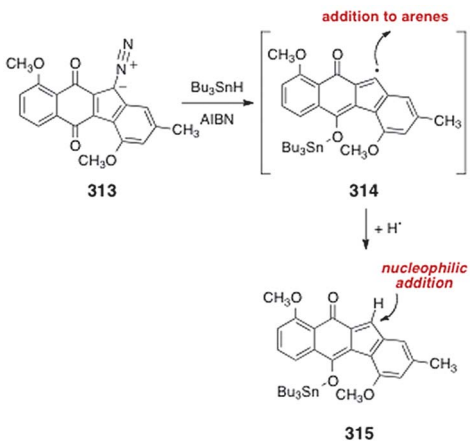

Scheme 59 Reaction pathway for dimethylprekinamycin (**313**) established by Feldman and Eastman.

a biological nucleophile to the diazo function, or alternatively, by formation of vinyl radicals *via* loss of dinitrogen from nucleophilic addition products (*e.g.*, **310**).

Feldman and Eastman have provided convincing evidence that the kinamycins form reactive vinyl radical and *ortho*-quinone methide intermediates under reducing conditions (Scheme 59).[121] The authors demonstrated that the alkenyl radical **314** is generated when the model substrate dimethyl prekinamycin (**313**) is exposed to reductants, such as tri-*n*-butyltin hydride. Products that may arise from addition of this radical (**314**) to aromatic solvents (benzene, anisole, and benzonitrile) were isolated. The *ortho*-quinone methide **315** was also formed, presumably by hydrogen atom abstraction by **314**. Alkylation products derived from nucleophilic addition to **315** were isolated. Accordingly, it was proposed that the kinamycins and lomaiviticins may exert their cytotoxic effects by generation of free radical or electrophilic *ortho*-quinone methide intermediates, following reductive activation. In a separate study, Skibo and co-workers examined the reduction of a series of prekinamycin analogs (Scheme 60).[122] It was established that catalytic hydrogenation of prekinamycin derivatives (**316**) forms *ortho*-quinone methide intermediates, such as **317**. Interestingly, these *ortho*-quinone methides were found to be in equilibrium with their keto tautomers (**318**), and the position of equilibrium was shown to be substituent-dependent. Prekinamycin analogs that exhibited the most stable *ortho*-quinone methide tautomers were found to be the most cytotoxic, suggesting these intermediates may be involved in the biological effects of the kinamycins and lomaiviticins.

Finally, in 1977, Moore proposed a novel mode of reactivity for kinamycin C (**3**, Scheme 61).[123] Moore originally formulated this postulate using the cyanocarbazole structure of the kinamycins. It is shown here for the corrected structure of kinamycin C (**3**). Reduction of kinamycin C (**3**) to the hydroquinone, followed by elimination of acetic acid, was postulated to form the vinylogous *ortho*-quinone methide **320**. This species may then eliminate a second equivalent of acetic acid, to form the double quinone methide **321**. It was proposed that both **320** and **321** may incorporate biological nucleophiles, leading to cell death.

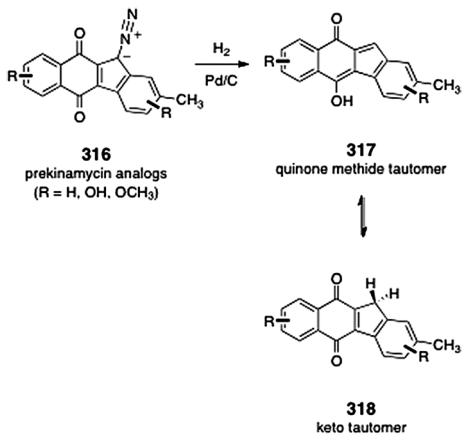

Scheme 60 Diazofluorene reduction and tautomeric equilibria observed by Skibo and co-workers.

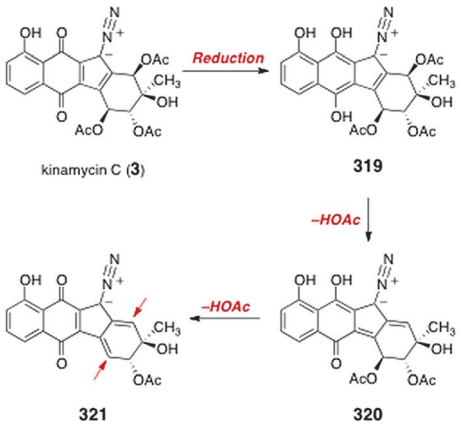

Scheme 61 Moore's proposal for the bioreductive activation of kinamycin C (**3**).

9 Related metabolites

9.1 Introduction

Many interesting metabolites related to the kinamycins and lomaiviticins have been isolated. A recent review of diazo-containing natural products, by Nawrat and Moody,[17] contains a comprehensive overview of naturally-occurring diazo compounds. A selection of related metabolites, which lack a diazo group, are discussed below.

9.2 Momofulvenones

Momofulvenones A (**322**) and B (**323**) were isolated as yellow salts (counter ion not specified) from the broth of *Streptomyces diastatochromogenes* by Zeeck and co-workers (Fig. 9).[124] The isolates displayed similar UV spectra under neutral or basic conditions, which lent support to their proposed anionic structures. The structures of the momofulvenones were ultimately corroborated by mass spectroscopy of chemical derivatives. Labeling studies established that the biosyntheses of the kinamycins and momofulvenones follow similar pathways. The momfulvenones are not reported to possess any biological activity, perhaps an indication of the importance of the diazo-function in the kinamycins and lomaiviticins.

9.3 Seongomycin

Seongomycin (**324**) was observed as a minor constituents of *Streptomyces murayamaensis*, and later isolated as the major metabolite in *Streptomyces lividans* transformed by the kinamycin gene cluster (Fig. 10).[125] Although seongomycin (**324**) was not observed from the wild type strain, it contained the characteristic 6,6,5,6 tetracyclic scaffold of the diazofluorene natural products, and appears to be a simple adduct of *N*-acetyl

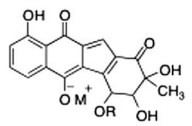

Fig. 9 Structures of momfulvenones A (**322**) and B (**323**).

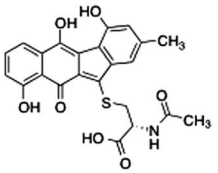

seongomycin (**324**)

Fig. 10 Structure of seongomycin (**324**).

cysteine. The side chain was established by NMR and FAB-MS analysis. The authors subsequently confirmed this structure *via* the biosynthetic incorporation of [1,2-$^{13}C_2$]acetate units. Incorporation of a cysteine unit is rare in polyketide metabolites from *Streptomyces*.

10 Conclusion and outlook

We have attempted in this review to compile the literature related to the kinamycins and lomaiviticins in one location to aid researchers in this exciting area. Although much progress has been made, several significant issues remain unresolved. First and foremost, the lomaiviticins have not yet succumbed to total synthesis, and their absolute stereochemistry remains unknown. Second, although a mounting body of evidence suggests the kinamycins and lomaiviticins are reductively-activated, a clear understanding of the molecular mechanisms underlying the cytotoxic effects of these compounds has not yet been obtained. Additionally, the biological target of these molecules has not been unequivocally established: although they have demonstrated DNA-cleaving abilities, the studies of Hasinoff and Dmitrienko seem to suggest one or more protein targets may exist. An intriguing possibility is that the molecules may be multipotent, that is, they may exert their cytotoxic effects through multiple mechanisms of action. Finally, the structural features of the lomaiviticins that impart such high levels of cytotoxicity to these metabolites have not been identified. Many of these issues are uniquely addressable by chemical synthesis, and future synthetic and chemical biological studies will bring resolution to these important questions.

Note added in proof

The synthesis of the epoxykinamycin FL-120B′ (**325**, Fig. 11)[10,11] was recently reported by Scully and Porco.[126]

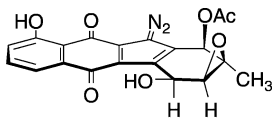

(–)-FL-120B′ (**325**)

Fig. 11 The structure of the epoxykinamycin derivative (–)-FL-120B′ (**325**).

11 References and notes

1 The producing strain of the lomaiviticins was originally classified as *Micromonospora*. This strain has subsequently been reclassified as *Salinispora*. Personal communication from Jeffrey Janso, 2011.

2 S. Ito, T. Matsuya, S. Ōmura, M. Otani and A. Nakagawa, *J. Antibiot.*, 1970, **23**, 315–317.

3 T. Hata, S. Ōmura, Y. Iwai, A. Nakagawa and M. Otani, *J. Antibiot.*, 1971, **24**, 353–359.

4 S. Ōmura, A. Nakagawa, H. Yamada, T. Hata, A. Furusaki and T. Watanabe, *Chem. Pharm. Bull.*, 1971, **19**, 2428–2430.

5 S. Ōmura, A. Nakagawa, H. Yamada, T. Hata and A. Furusaki, *Chem. Pharm. Bull.*, 1973, **21**, 931–940.

6 M. C. Cone, P. J. Seaton, K. A. Halley and S. J. Gould, *J. Antibiot.*, 1989, **42**, 179–188.

7 K. Isshiki, T. Sawa, H. Naganawa, N. Matsuda, S. Hattori, M. Hamada, T. Takeuchi, M. Oosono, M. Ishizuka, Z. Yang, B. Zhu and W. Xu, *J. Antibiot.*, 1989, **42**, 467–469.

8 P. J. Seaton and S. J. Gould, *J. Antibiot.*, 1989, **42**, 189–197.

9 T. A. Smitka, R. Bonjouklian, T. J. Perun, A. H. Hunt, R. S. Foster, J. S. Mynderse and R. C. Yao, *J. Antibiot.*, 1992, **45**, 581–583.

10 H.-C. Lin, S.-C. Chang, N.-L. Wang and L.-R. Chang, *J. Antibiot.*, 1994, **47**, 675–680.

11 H.-C. Lin, S.-C. Chang, N.-L. Wang and L.-R. Chang, *J. Antibiot.*, 1994, **47**, 681–687.

12 H. He, W. D. Ding, V. S. Bernan, A. D. Richardson, C. M. Ireland, M. Greenstein, G. A. Ellestad and G. T. Carter, *J. Am. Chem. Soc.*, 2001, **123**, 5362–5363.

13 W. G. Overend, C. W. Rees and J. S. Sequeira, *J. Chem. Soc.*, 1962, 3429–3440.

14 R. H. Shoemaker, *Nat. Rev. Cancer*, 2006, **6**, 813–823.

15 S. J. Gould, *Chem. Rev.*, 1997, **97**, 2499–2510.

16 J. Marco-Contelles and M. T. Molina, *Curr. Org. Chem.*, 2003, **7**, 1433–1442.

17 C. C. Nawrat and C. J. Moody, *Nat. Prod. Rep.*, 2011, **28**, 1426–1444.

18 D. P. Arya, *Top. Heterocycl. Chem.*, 2006, **2**, 129–152.

19 A. Furusaki, M. Matsui, T. Watanabe, S. Ōmura, A. Nakagawa and T. Hata, *Isr. J. Chem.*, 1972, **10**, 173–187.

20 K. Ajisaka, H. Takeshima and S. Ōmura, *J. Chem. Soc., Chem. Commun.*, 1976, 571.

21 P. J. Seaton and S. J. Gould, *J. Am. Chem. Soc.*, 1988, **110**, 5912–5914.

22 G. I. Dmitrienko, K. E. Nielsen, C. Steingart, S. M. Ngai, J. M. Willson and G. Weeratunga, *Tetrahedron Lett.*, 1990, **31**, 3681–3684.

23 A. M. Echavarren, N. Tamayo and M. C. Paredes, *Tetrahedron Lett.*, 1993, **34**, 4713–4716.

24 S. J. Gould, N. Tamayo, C. R. Melville and M. C. Cone, *J. Am. Chem. Soc.*, 1994, **116**, 2207–2208.

25 S. Mithani, G. Weeratunga, N. J. Taylor and G. I. Dmitrienko, *J. Am. Chem. Soc.*, 1994, **116**, 2209–2210.

26 D. R. Schroeder, K. L. Colson, S. E. Klohr, M. S. Lee, J. A. Matson, L. S. Brinen and J. Clardy, *J. Antibiot.*, 1996, **49**, 865–872.

27 S. J. Gould and C. R. Melville, *Bioorg. Med. Chem. Lett.*, 1995, **5**, 51–54.

28 S. J. Gould, C. R. Melville, M. C. Cone, J. Chen and J. R. Carney, *J. Org. Chem.*, 1997, **62**, 320–324.

29 N. Chen, M. B. Carriere, R. S. Laufer, N. J. Taylor and G. I. Dmitrienko, *Org. Lett.*, 2008, **10**, 381–384.

30 S. J. Gould, T. O'Hare, P. Seaton, J. Soodsma and Z. Tang, *Bioorg. Med. Chem.*, 1996, **4**, 987–994.

31 X. Lei and J. A. Porco, *J. Am. Chem. Soc.*, 2006, **128**, 14790–14791.

32 For a review, see: S. P. Roche and J. A. Porco, *Angew. Chem., Int. Ed.*, 2011, **50**, 4068–4093.

33 Y. Hu, C. Li, B. A. Kulkarni, G. Strobel, E. Lobkovsky, R. M. Torczynski and J. A. Porco, *Org. Lett.*, 2001, **3**, 1649–1652.

34 V. K. Aggarwal, A. Mereu, G. J. Tarver and R. McCague, *J. Org. Chem.*, 1998, **63**, 7183–7189.

35 C. L. Elston, R. F. W. Jackson, S. J. F. MacDonald and P. J. Murray, *Angew. Chem., Int. Ed. Engl.*, 1997, **36**, 410–412.

36 C. Li, E. A. Pace, M.-C. Liang, E. Lobkovsky, T. D. Gilmore and J. A. Porco, *J. Am. Chem. Soc.*, 2001, **123**, 11308–11309.

37 C. Li, R. P. Johnson and J. A. Porco, *J. Am. Chem. Soc.*, 2003, **125**, 5095–5106.

38 M. E. Jung and J. A. Hagenah, *J. Org. Chem.*, 1983, **48**, 5359–5361.

39 H. Azizian, C. Eaborn and A. Pidcock, *J. Organomet. Chem.*, 1981, **215**, 49–58.

40 M. Caron and K. B. Sharpless, *J. Org. Chem.*, 1985, **50**, 1557–1560.

41 M. E. Furrow and A. G. Myers, *J. Am. Chem. Soc.*, 2004, **126**, 5436–5445.
42 M. E. Furrow and A. G. Myers, *J. Am. Chem. Soc.*, 2004, **126**, 12222–12223.
43 Y. Kitani, A. Morita, T. Kumamoto and T. Ishikawa, *Helv. Chim. Acta*, 2002, **85**, 1186–1195.
44 T. Kumamoto, Y. Kitani, H. Tsuchiya, K. Yamaguchi, H. Seki and T. Ishikawa, *Tetrahedron*, 2007, **63**, 5189–5199.
45 S. W. Heinzman and J. R. Grunwell, *Tetrahedron Lett.*, 1980, **21**, 4305–4308.
46 K. C. Nicolaou, T. Montagnon and P. S. Baran, *Angew. Chem., Int. Ed.*, 2002, **41**, 993–996.
47 T. J. Donohoe, K. Blades, P. R. Moore, M. J. Waring, J. J. G. Winter, M. Helliwell, N. J. Newcombe and G. Stemp, *J. Org. Chem.*, 2002, **67**, 7946–7956.
48 D. A. Evans, K. T. Chapman and E. M. Carreira, *J. Am. Chem. Soc.*, 1988, **110**, 3560–3578.
49 P. Jacob, P. S. Callery, A. T. Shulgin and N. Castagnoli, *J. Org. Chem.*, 1976, **41**, 3627–3629.
50 K. C. Nicolaou, H. Li, A. L. Nold, D. Pappo and A. Lenzen, *J. Am. Chem. Soc.*, 2007, **129**, 10356–10357.
51 G. Giuffredi, C. Bobbio and V. r. Gouverneur, *J. Org. Chem.*, 2006, **71**, 5361–5364.
52 C. R. Johnson, J. P. Adams, M. P. Braun, C. B. W. Senanayake, P. M. Wovkulich and M. R. Uskokovic, *Tetrahedron Lett.*, 1992, **33**, 917–918.
53 M. G. Banwell, B. D. Kelly, O. J. Kokas and D. W. Lupton, *Org. Lett.*, 2003, **5**, 2497–2500.
54 M. S. Kerr, J. Read de Alaniz and T. Rovis, *J. Am. Chem. Soc.*, 2002, **124**, 10298–10299.
55 M. S. Kerr, J. Read de Alaniz and T. Rovis, *J. Org. Chem.*, 2005, **70**, 5725–5728.
56 G. A. Molander and G. Hahn, *J. Org. Chem.*, 1986, **51**, 1135–1138.
57 For a review, see: G. A. Molander, *Chem. Rev.*, 1992, **92**, 29–68.
58 C. M. Woo, L. Lu, S. L. Gholap, D. R. Smith and S. B. Herzon, *J. Am. Chem. Soc.*, 2010, **132**, 2540–2541.
59 H. C. Kolb, M. S. VanNieuwenhze and K. B. Sharpless, *Chem. Rev.*, 1994, **94**, 2483–2547.
60 H. J. Reich, I. L. Reich and J. M. Renga, *J. Am. Chem. Soc.*, 1973, **95**, 5813–5815.
61 K. B. Sharpless, R. F. Launer and A. Y. Teranishi, *J. Am. Chem. Soc.*, 1973, **95**, 6137–6139.
62 A. B. Charette, R. P. Wurz and T. Ollevier, *J. Org. Chem.*, 2000, **65**, 9252–9254.
63 W. v. E. Doering and C. H. DePuy, *J. Am. Chem. Soc.*, 1953, **75**, 5955–5957.
64 K. C. Nicolaou, R. M. Denton, A. Lenzen, D. J. Edmonds, A. Li, R. R. Milburn and S. T. Harrison, *Angew. Chem., Int. Ed.*, 2006, **45**, 2076–2081.
65 G.-q. Lin and R. Hong, *J. Org. Chem.*, 2001, **66**, 2877–2880.
66 T. Imamoto, N. Takiyama, K. Nakamura, T. Hatajima and Y. Kamiya, *J. Am. Chem. Soc.*, 1989, **111**, 4392–4398.
67 W. Zhang, A. Baranczak and G. A. Sulikowski, *Org. Lett.*, 2008, **10**, 1939–1941.
68 J. E. Audia, L. Boisvert, A. D. Patten, A. Villalobos and S. J. Danishefsky, *J. Org. Chem.*, 1989, **54**, 3738–3740.
69 E. S. Krygowski, K. Murphy-Benenato and M. D. Shair, *Angew. Chem., Int. Ed.*, 2008, **47**, 1680–1684.
70 H. G. Lee, J. Y. Ahn, A. S. Lee and M. D. Shair, *Chem.–Eur. J.*, 2010, **16**, 13058–13062.
71 H. H. Wasserman and G. M. Lee, *Tetrahedron Lett.*, 1994, **35**, 9783–9786.
72 D. A. Evans, K. T. Chapman and J. Bisaha, *J. Am. Chem. Soc.*, 1988, **110**, 1238–1256.
73 D. A. Evans, J. S. Tedrow, J. T. Shaw and C. W. Downey, *J. Am. Chem. Soc.*, 2002, **124**, 392–393.
74 G. A. Kraus and H. Sugimoto, *Tetrahedron Lett.*, 1978, **19**, 2263–2266.
75 F. M. Hauser and R. P. Rhee, *J. Org. Chem.*, 1978, **43**, 178–180.
76 K. C. Nicolaou, A. L. Nold and H. Li, *Angew. Chem., Int. Ed.*, 2009, **48**, 5860.
77 S. B. Herzon, L. Lu, C. M. Woo and S. L. Gholap, *J. Am. Chem. Soc.*, 2011, **133**, 7260–7263.
78 S. Evans, A. Hamnett, A. F. Orchard and D. R. Lloyd, *Faraday Discuss. Chem. Soc.*, 1972, **54**, 227–250.
79 J. R. Bryant, J. E. Taves and J. M. Mayer, *Inorg. Chem.*, 2002, **41**, 2769–2776.
80 R. W. Burg, B. M. Miller, E. E. Baker, J. Birnbaum, S. A. Currie, R. Hartman, Y.-L. Kong, R. L. Monaghan, G. Olson, I. Putter, J. B. Tunac, H. Wallick, E. O. Stapley, R. Oiwa and S. Ōmura, *Antimicrob. Agents Chemother.*, 1979, **15**, 361–367.
81 T. W. Miller, L. Chaiet, D. J. Cole, L. J. Cole, J. E. Flor, R. T. Goegelman, V. P. Gullo, H. Joshua, A. J. Kempf, W. R. Krellwitz, R. L. Monaghan, R. E. Ormond, K. E. Wilson, G. Albers-Schonberg and I. Putter, *Antimicrob. Agents Chemother.*, 1979, **15**, 368–371.
82 K. S. Lam, G. A. Hesler, D. R. Gustavson, R. L. Berry, K. Tomita, J. L. MacBeth, J. Ross, D. Miller and S. Forenza, *J. Antibiot.*, 1996, **49**, 860–864.
83 F. Blindenbacher and T. Reichstein, *Helv. Chim. Acta*, 1948, **31**, 2061–2064.
84 G. Berti, G. Catelani, F. Colonna and L. Monti, *Tetrahedron*, 1982, **38**, 3067–3072.
85 P. G. M. Wuts and S. S. Bigelow, *J. Org. Chem.*, 1983, **48**, 3489–3493.
86 D. Ravi, V. R. Kulkarni and H. B. Mereyala, *Tetrahedron Lett.*, 1989, **30**, 4287–4290.
87 R. L. Tolman and L. H. Peterson, *Carbohydr. Res.*, 1989, **189**, 113–122.
88 M. J. Ford and S. V. Ley, *Synlett*, 1990, 771–772.
89 M. W. Bredenkamp, C. W. Holzapfel and F. Toerien, *Synth. Commun.*, 1992, **22**, 2459–2477.
90 X. Y. Zhao, M. Ono, H. Akita and Y. M. Chi, *Chin. Chem. Lett.*, 2006, **17**, 730–732.
91 D. Hou and T. L. Lowary, *Carbohydr. Res.*, 2009, **344**, 1911–1940.
92 W. J. Morris and M. D. Shair, *Org. Lett.*, 2008, **11**, 9–12.
93 W. J. Morris and M. D. Shair, *Tetrahedron Lett.*, 2010, **51**, 4310–4312.
94 R. L. Halcomb, M. D. Wittman, S. H. Olson, S. J. Danishefsky, J. Golik, H. Wong and D. Vyas, *J. Am. Chem. Soc.*, 1991, **113**, 5080–5082.
95 V. G. S. Box, *Heterocycles*, 1982, **19**, 1939–1966.
96 R. R. Schmidt and J. Michel, *Tetrahedron Lett.*, 1984, **25**, 821–824.
97 R. R. Schmidt, *Angew. Chem., Int. Ed. Engl.*, 1986, **25**, 212–235.
98 W. Klotz and R. R. Schmidt, *Liebigs Ann. Chem.*, 1993, 683–690.
99 S. L. Gholap, C. M. Woo, P. C. Ravikumar and S. B. Herzon, *Org. Lett.*, 2009, **11**, 4322–4325.
100 Z.-X. Wang, Y. Tu, M. Frohn, J.-R. Zhang and Y. Shi, *J. Am. Chem. Soc.*, 1997, **119**, 11224–11235.
101 S.-i. Hashimoto, A. Sano, H. Sakamoto, M. Hakajima, Y. Yanagiya and S. Ikegami, *Synlett*, 1995, 1271–1273.
102 Y. Guo and G. A. Sulikowski, *J. Am. Chem. Soc.*, 1998, **120**, 1392–1397.
103 R. Pongdee, B. Wu and G. A. Sulikowski, *Org. Lett.*, 2001, **3**, 3523–3525.
104 G. H. Posner and S. R. Haines, *Tetrahedron Lett.*, 1985, **26**, 5–8.
105 F. M. Hauser and M. Zhou, *J. Org. Chem.*, 1996, **61**, 5722–5722.
106 D. Mal and N. K. Hazra, *Tetrahedron Lett.*, 1996, **37**, 2641–2642.
107 V. B. Birman, Z. F. Zhao and L. Guo, *Org. Lett.*, 2007, **9**, 1223–1225.
108 S. Kimura, S. Kobayashi, T. Kumamoto, A. Akagi, N. Sato and T. Ishikawa, *Helv. Chim. Acta*, 2011, **94**, 578–591.
109 W. Liu, M. Buck, N. Chen, M. Shang, N. J. Taylor, J. Asoud, X. Wu, B. B. Hasinoff and G. I. Dmitrienko, *Org. Lett.*, 2007, **9**, 2915–2918.
110 P. J. Proteau, Y. Li, J. Chen, R. T. Williamson, S. J. Gould, R. S. Laufer and G. I. Dmitrienko, *J. Am. Chem. Soc.*, 2000, **122**, 8325–8326.
111 S. Kim and K. H. Ahn, *J. Org. Chem.*, 1984, **49**, 1717–1724.
112 S.-i. Mohri, M. Stefinovic and V. Snieckus, *J. Org. Chem.*, 1997, **62**, 7072–7073.
113 K. Shin-ya, K. Furihata, Y. Teshima, Y. Hayakawa and H. Seto, *Tetrahedron Lett.*, 1992, **33**, 7025–7028.
114 H. Koyama and T. Kamikawa, *J. Chem. Soc., Perkin Trans. 1*, 1998, 203–210.
115 T. E. Ballard and C. Melander, *Tetrahedron Lett.*, 2008, **49**, 3157–3161.
116 C. L. Heinecke and C. Melander, *Tetrahedron Lett.*, 2010, **51**, 1455–1458.

117 W. Zeng, T. E. Ballard, A. G. Tkachenko, V. A. Burns, D. L. Feldheim and C. Melander, *Bioorg. Med. Chem. Lett.*, 2006, **16**, 5148–5151.
118 K. A. O'Hara, X. Wu, D. Patel, H. Liang, J. C. Yalowich, N. Chen, V. Goodfellow, O. Adedayo, G. I. Dmitrienko and B. B. Hasinoff, *Free Radical Biol. Med.*, 2007, **43**, 1132–1144.
119 D. P. Arya and D. J. Jebaratnam, *J. Org. Chem.*, 1995, **60**, 3268–3269.
120 R. S. Laufer and G. I. Dmitrienko, *J. Am. Chem. Soc.*, 2002, **124**, 1854–1855.
121 K. S. Feldman and K. J. Eastman, *J. Am. Chem. Soc.*, 2006, **128**, 12562–12573.
122 O. Khdour and E. B. Skibo, *Org. Biomol. Chem.*, 2009, **7**, 2140–2154.
123 H. W. Moore, *Science*, 1977, **197**, 527–532.
124 C. Volkmann, E. Rössner, M. Metzler, H. Zähner and A. Zeeck, *Liebigs Ann.*, 1995, **1995**, 1169–1172.
125 J. R. Carney, S.-T. Hong and S. J. Gould, *Tetrahedron Lett.*, 1997, **38**, 3139–3142.
126 S. S. Scully and J. A. Porco, *Angew. Chem., Int. Ed. Engl.*, 2011, **50**, 9722–9726.

